ELSEVIER

Powder Technology 104 (1999) 1–28

POWDER TECHNOLOGY

A comparative experimental study of five multivariable control strategies applied to a grinding plant

Manuel Duarte [a,*], Florencio Sepúlveda [a], Alejandro Castillo [a], Angel Contreras [a], Vanel Lazcano [a], Patricio Giménez [b], Luis Castelli [b]

[a] *Department of Electrical Engineering, University of Chile, Av. Tupper 2007, Casilla 412-3, Santiago, Chile*
[b] *CODELCO-Chile, División Andina, Saladillo, Chile*

Received 4 August 1997; received in revised form 30 September 1998; accepted 30 September 1998

Abstract

This paper deals with the implementation of five multivariable adaptive, as well as classical, control strategies in an industrial grinding plant. The extended horizon, pole-placement, model reference, direct Nyquist Array and sequential loop closing algorithms were studied and implemented at CODELCO-Andina's copper grinding plant, with each of them delivering good performance. The 2×2 system chosen to be controlled has the percentage of solids (percentage of $+65$ mesh) fed to the hydrocyclones and the level of the sump as output variables, and the water flow added to the sump and the pump speed as input variables. The adaptive extended horizon algorithm performs the best, although all five strategies considerably improve the actual operation of the plant which consists of only one control loop. After a comparison amongst the control strategies, a brief economic impact analysis is performed to support the claim that multivariable control algorithms substantially improve the operation of the grinding plant, maintaining the percentage of solids (percentage over mesh 65) around a pre-specified value (optimal for practical purposes); thus obtaining interesting economic benefits.

Keywords: Grinding; Multivariable control; Plant control; Mineral industry

1. Introduction

Over the last 20 years, great effort has been dedicated to the study and implementation of control strategies in mineral concentrator plants. Grinding is a fundamental operation process in reducing mineral particle size, but the energy required by the mill motors is high, making grinding a very expensive process. From previous experience in studying this type of process, it is possible to obtain substantial improvements in operation efficiency, and thereby significant reductions in production costs, if grinding plant is operated in an appropriate form.

Controlling mineral processing plants is an art. Due to the particular nature of each process and the differences in mineral characteristics, solutions regarding the system configuration as well as the type of control algorithms have to be obtained for each plant. The control of grinding processes is extremely complex for two basic reasons. First, the large number of variables involved have a high degree of interaction among them. This means that if control of one output variable is attempted with one input variable, the other output variable will, more likely than not, be affected in an undesired fashion. Secondly, the existence of unmodeled dynamics, time-varying parameters, noisy measurements, bias in the measurements, large delays, important differences in the values of the time constants, nonlinearities, etc. are some of the other difficulties encountered in the control. The first aspect is solved by implementing multivariable control strategies so that more than one variable is controlled at once, introducing some degree of decoupling among them. The second aspect is taken into account by incorporating some degree of adaptation in the control system. Thus, this poses a reasonable problem for classical and adaptive multivariable control techniques.

Classical multivariable control techniques, such as the Inverse Nyquist Array (INA), the Direct Nyquist Array (DNA), sequential loop closing (SLC) [1,10], etc. do not consider the time variations of the process parameters and the controller parameters must be frequently retuned manually.

* Corresponding author. E-mail: mduartem@cec.uchile.cl

0032-5910/99/$ - see front matter © 1999 Elsevier Science S.A. All rights reserved.
PII: S0032-5910(98)00210-1

Adaptive multivariable control techniques, such as multivariable extended horizon adaptive control (MEHAC) [2,44], multivariable pole-placement adaptive control (MPPAC) [3] and multivariable model reference adaptive control (MMRAC) [4], on the other hand, have automatic adjustment mechanisms of the controller parameters according to variations in the process and its environment.

Numerous applications of the multivariable control of grinding plants have been reported in control literature, both at simulation, as well as experimental levels. However, very few of these currently operate in industry [6]. Hulbert [7] shows the dynamics of the grinding process to be highly interactive, and the application of a multivariable control scheme to be necessary. Metzner and McLeod [5] used phenomenological knowledge of the plant in order to reduce the number of estimated parameters from a practically intractable value (95) to an acceptable level (35), and the resulting designed controller exhibited good simulation performance. In Ref. [8], the effectiveness of multivariable adaptive control is proven, as compared with a classical PID controller, resulting from the nonlinear nature of the grinding plant. In Ref. [9], on the other hand, it is concluded that the design of a multivariable predictive controller is simpler than the design of a controller based on the Inverse Nyquist Array.

So called classical multivariable control has been used extensively in a great variety of processes. One of the most interesting processes in the application of these techniques is the grinding plant, due to the high degree of interaction amongst the variables. There are some pioneer groups in the application of these techniques, such as The Division of Measurement and Control of the Council of Mining Technology of South Africa (MINTEK) in which multivariable control of industrial mill circuits has been applied [27–29]. Also, the Finnish Center of Technical Research and Outokumpu Oy, have instigated similar developments [30,31]. These applications have mainly been in gold, coal and copper mines. Other results of interest in this field, at an industrial scale, are reported in Refs. [36,37]. Industrial implementation of the INA technique has received considerable attention [27,28,36,45–47] in several types of mines and grinding circuits.

At present, all of the concentrator plants in Chile have some degree of automation. However, the control strategies in operation are, for the most part, of stabilizing nature and many of them are steady-state control strategies, i.e., they transfer the processes in a slow fashion from one stationary state to another. One of the first experiences of multivariable control in Chile was developed in 1988 [32], employing the INA method in a real grinding plant. Previous work, during the 1970s, was oriented at reducing the effects of perturbations on a linearized multivariable system [33].

The main objective of the work presented here is to report the results obtained from the application of five multivariable control strategies (adaptive and classical) to a conventional grinding plant at experimental level. The plant chosen for the study and implementation is the concentrator section of CODELCO Chile-Andina. These strategies are local or stabilizing control and form part of a more general control strategy for the plant. The controlled variables are the percentage of solids (density) of the pulp fed to the hydrocyclones and the level of the sump, while the manipulated variables are the flow of water to the sump and the pump speed. (See Fig. 1).

The control schemes selected for this study are three adaptive techniques and two classical techniques. MEHAC has been used in its incremental version [2,12,44], with a model of the plant formulated in state space using the canonical observable form. MPPAC has been used in its incremental version [3,5,12,16] and has two fundamental stages: one is the resolution of the Bezout Identity and the other is the minimization of coupling between the references and the non-corresponding outputs. The MMRAC used in this study is formulated in its incremental version [4,12] and drives the control error to zero indirectly as the identification error tends to zero. The controller parameters are computed algebraically using a model of the plant under control.

As far as classical multivariable techniques are concerned, the method of multivariable direct Nyquist array control (MDNAC) [1,10] and the method of multivariable sequential loop closing control (MSLCC) [1] were used.

Finally, a comparison is made of the different techniques implemented for controlling the grinding plant, drawing the conclusion that the adaptive techniques present better behavior than classical ones, and among the adaptive schemes the extended horizon is the most promising. Towards the end of the paper a brief economic impact analysis is performed in support of the claim that multivariable control algorithms substantially improve the operation of the grinding plant, maintaining the percentage of solids (percentage over mesh 65) around a pre-specified value (optimal for practical purposes), thus obtaining interesting economic benefits.

2. The grinding process

The grinding plant of the CODELCO-Andina concentrator consists of three parallel and identical sections, except for the instrumentation available in each section, denoted by A, B and C. Each one comprises a rod mill in open circuit and three identical lines of ball mills in closed inverse circuit with hydrocyclones (see Fig. 1).

The product of the crushing enters the grinding stage via three conveyor belts, one for each section, which have weightmeters registering the mineral tonnage to be processed in each section. The belt discharge feeds the rod mill where the necessary water for the operation is added. At this point, lime is added in order to regulate the pH at the flotation stage. Also, approximately 50% of the collector is added. The pulp discharged by the rod mill, contain-

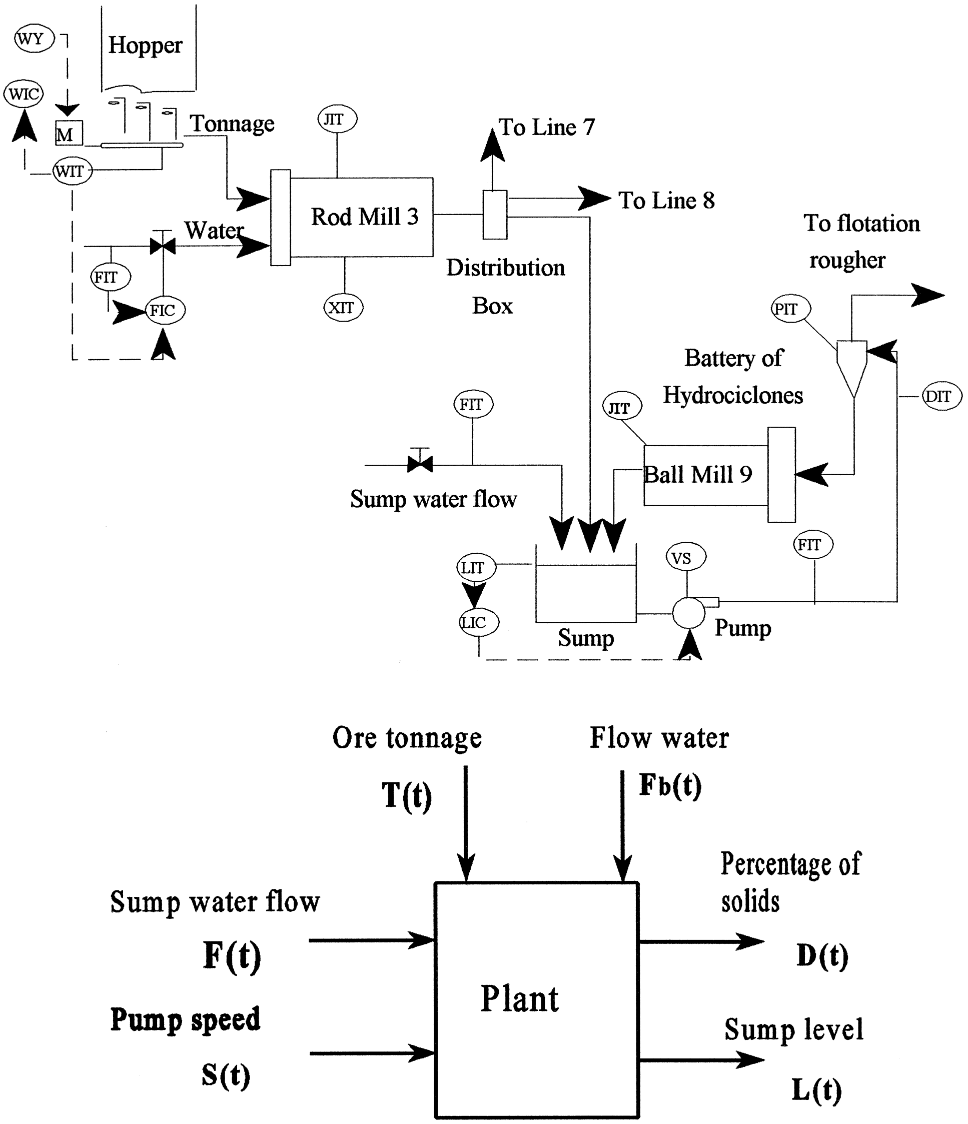

Fig. 1. Grinding section of CODELCO-Andina concentrator.

ing 81% solids, is routed to the three lines (not necessarily equal) by means of a distributing box. Each one is sent through pipes to the sump from where the pumps feed the hydrocyclones, operating in inverse circuit with the respective ball mill. In the hydrocyclones, the particles follow a helical trajectory due to the effect of the centrifugal forces and gravity. A vortex of low pressure is created that produces a column of upward air. Since the thick particles possess higher mass, they are led to the periphery, falling toward the discharge of the hydrocyclone. In turn, the fine particles located near the center of the hydrocyclone, are discharged through the overflow. The hydrocyclone discharge feeds the ball mill. The discharge of these mills goes to the sump feeding the hydrocyclones. The hydrocyclones' overflow constitutes the final product of the grinding process and is sent onto flotation. This product is of an average particle size of 42% -200 mesh (74 μ) and 25% $+65$ mesh (212 μ). Fig. 1 depicts the configuration of Section C of the grinding plant of the CODELCO-Andina concentrator.

For this study, the plant is defined by a 2×2 multivariable system, where the outputs are the percentage of solids (density) in the pulp-feeding hydrocyclones, denoted as $D(t)$ and the level of the sump $L(t)$, and the inputs are the flow of water to the sump $F(t)$ and the pump speed $S(t)$. The remaining input variables to the grinding plant (measured or unmeasured) affecting these two output variables are considered perturbations, as well as any other variation in the characteristics of the process. By way of example, some of these perturbations include: variations in the hardness of the mineral, variations in the input size distribution [11], nonhomogenous distribution of the pulp in the distribution box, variations in the feed tonnage to the rod mill, starting and stopping of ball mills, variations in the pressure of the water fed to the sump, and changes in the process dynamics.

It has been both theoretically and experimentally demonstrated that a very good correlation exists between the percentage of solids (density) in the pulp fed to hydrocyclones and the particle size in the overflow of the hydrocyclones. In several tests carried out for this study, correlation indexes of $r = 0.85$ and higher were found [12]. The control objective in this case will be to maintain the particle size in the hydrocyclones' overflow (the percentage of solids (density) in the feeding to hydrocyclones), as constant as possible around a value specified by the flotation stage, so that the recovery of mineral is as high as possible, according to the operation conditions of the plant.

3. Brief description of multivariable control algorithms

The multivariable control strategies used in the study are briefly described in this section.

3.1. Multivariable extended horizon adaptive control (MEHAC)

The multivariable extended horizon indirect adaptive control technique [2,44], with its corresponding modifications and extensions as mentioned in Ref. [12] has been used in this study. This algorithm is very simple, minimizing n cost functions (assuming an n-input n-output plant) that simply consist of the square of each component of the difference vector between output and reference. Each of these differences is computed in a pre-specified future time called the control horizon, that can differ for each component of the output vector. Each control horizon is greater or equal to the greatest delay between the respective component of the output vector and all the elements of the input vector.

Calculation of the control law is based on the values of the plant model parameters formulated in a state space structure in canonical observable form, that avoids having to estimate the state of the plant. The model of the plant has the following structure:

$$\mathbf{X}(t+1) = \mathbf{A}\mathbf{X}(t) + \mathbf{B}\boldsymbol{u}(t-k),$$
$$\boldsymbol{y}(t) = \mathbf{C}\mathbf{X}(t)$$

where k represents the delay between the input and the output, which are all assumed equal.

The parameters of the model are estimated using multivariable recursive least squares with UD factorization [14] of the covariance matrix and with a variable forgetting factor [15]. From the incremental version of the control and identification algorithms, a controller with integral action is obtained.

For a second-order system of two inputs and two outputs, matrices $\mathbf{A}$, $\mathbf{B}$, $\mathbf{C}$ of 2×2 and unit controllability indexes in the observable canonical form, the equations describing the model of the plant are [12]

$$y_1(t) = a_1^{11} y_1(t-1) + a_1^{12} y_2(t-1) + b_1^{11} u_1(t-1) + b_1^{12} u_2(t-1)$$
$$y_2(t) = a_2^{21} y_1(t-1) + a_2^{22} y_2(t-1) + b_2^{21} u_1(t-1) + b_2^{22} u_2(t-1).$$

Defining the cost function

$$J_i = \left(r_i(t) - y_i(t+T_i)\right)^2, \qquad i = 1,2 \tag{1}$$

where T_1 and T_2 are the control horizons associated with each output variable and $\boldsymbol{r}(t)$ is the reference vector. The control law that minimizes Eq. (1) turns out to be [12]

$$\begin{aligned} \boldsymbol{\Delta} u_i(t) &= \boldsymbol{v}_i^{\mathrm{T}} \mathbf{D}(T_i)^{-1} \left[\boldsymbol{r}(t) - Y_i(t)\right], \qquad i = 1,2 \\ \mathbf{D}(T_i) &= \mathbf{C}\left\{\sum_{j=1}^{T_i} \mathbf{A}^{j-1}\right\}\mathbf{B}, \\ Y_i(t) &= \boldsymbol{y}(t) + \mathbf{C}\left\{\sum_{j=1}^{T_i} \mathbf{A}^{j}\mathbf{X}(t)\right\}. \end{aligned} \tag{2}$$

where $\boldsymbol{\Delta} = \mathbf{I} - \boldsymbol{z}^{-1}$ is the incremental operator and $\boldsymbol{v}_i$ is a unit vector with a 1 in the ith position.

3.2. Multivariable pole-placement adaptive control (MPPAC)

The incremental version [5] of the multivariable indirect adaptive pole-placement controller [3,16] has proved robust in controlling non minimum phase plants and systems with large delays. Moreover, different sampling periods may be chosen for each loop if necessary.

The algorithm minimizes a vectorial cost function of dimension n (in an n-input and n-output system), consisting of a linear combination of the input vector, the output vector and the reference vector. The weighting coefficients of the linear combination are simply matrices whose elements are polynomials in $\boldsymbol{z}^{-1}$. The values of the polynomial's coefficients need to be established in order to determine the necessary control actions, which is a two-stage process. First, the solution of the Bezout Identity to locate the closed loop poles is found and second, the minimization of the coupling between the off-diagonal input–output pairs is achieved.

Successful execution of the two above stages depends on the knowledge of the plant's model parameters. To solve this problem, the recursive least-squares algorithm is used with UD factorization of the covariance matrix [14] and with a variable forgetting factor [15]. A controller with integral action is obtained with the incremental version of the control and identification algorithms and the necessity of estimating the constant vector $\boldsymbol{d}$ in Eq. (3) is avoided. The incremental version's additional integrator enables us to eliminate the steady-state error.

Let us consider a model of a process of n-inputs and n-outputs described by:

$$\mathbf{A}(z^{-1})\boldsymbol{y}(t) = z^{-kij}\mathbf{B}(z^{-1})\boldsymbol{u}(t) + \mathbf{C}(z^{-1})\boldsymbol{e}(t) + \boldsymbol{d} \qquad (3)$$

where $\boldsymbol{y}(t)$, $\boldsymbol{u}(t)$, $\boldsymbol{e}(t)$ and $\boldsymbol{d} \in \Re^n$ are the output, input, noise and bias vectors, respectively. $\mathbf{A}(z^{-1})$, $\mathbf{C}(z^{-1})$ are monic and diagonal matrix operators of $n \times n$ and $\mathbf{B}(z^{-1})$ is a full matrix operator of $n \times n$. z^{-kij} operates on the ij element of matrix $\mathbf{B}(z^{-1})$ and represents a delay of magnitude k_{ij}.

The structure of the model can be rewritten as:

$$\mathbf{A}(z^{-1})\boldsymbol{\Delta y}(t) = z^{-kij}\mathbf{B}(z^{-1})\boldsymbol{\Delta u}(t) + \mathbf{C}(z^{-1})\boldsymbol{\Delta e}(t)$$

where $\boldsymbol{\Delta} = \mathbf{I} - z^{-1}$. Since matrices $\mathbf{A}(z^{-1})$ and $\mathbf{C}(z^{-1})$ are diagonal, only identification of n MISO models is necessary.

Let us define the following cost vectorial function [5]:

$$\boldsymbol{\phi}(t + k_{ii}) = \mathbf{C}^{-1}\left[z^{-(k_{ij}-k_{ii})}(\mathbf{EB} + \mathbf{CQ})\boldsymbol{\Delta u}(t) + \mathbf{F}\boldsymbol{y}(t) - \mathbf{CR}\boldsymbol{r}(t)\right] \qquad (4)$$

where $\mathbf{E}(z^{-1})$ and $\mathbf{F}(z^{-1})$ are two diagonal matrix operators of $n \times n$, solution of the equation:

$$\mathbf{PC} = \boldsymbol{\Delta}\mathbf{AE} + z^{-k_{ii}}\mathbf{F}$$

The polynomial elements of the matrices $\mathbf{E}$ and $\mathbf{F}$ are of degrees n_{ei} and n_{fi} defined as:

$$n_{ei} = k_{ii} - 1$$

$$n_{fi} = \begin{cases} n_{ai} + n_{ci} - k_{ii} + 1 & \text{if } k_{ii} \le n_{ci} + 1 \\ n_{ai} & \text{if } k_{ii} > n_{ci} + 1 \end{cases}$$

$\mathbf{P}(z^{-1})$ and $\mathbf{R}(z^{-1})$ are two monic and diagonal matrices of $n \times n$, and $\mathbf{Q}(z^{-1})$ is a full polynomial matrix of $n \times n$. $\mathbf{P}$, $\mathbf{Q}$ and $\mathbf{R}$ are three matrices defined by the designer.

The control law that minimizes the cost function (4) is given by:

$$z^{-(k_{ij}-k_{ii})}\mathbf{S}\boldsymbol{\Delta u}(t) = \mathbf{F}\boldsymbol{y}(t) - \mathbf{CR}\boldsymbol{r}(t) \qquad (5)$$

where $\mathbf{S} = \mathbf{EB} + \mathbf{CQ}$. Matrix $\mathbf{S}$ can be written as $\mathbf{S} = \mathbf{S}_D + \mathbf{S}_{UL}$ where $\mathbf{S}_D$ is a diagonal matrix defined as $\mathbf{S}_D = \mathbf{EB}_D + \mathbf{CQ}_D$ and $\mathbf{S}_{UL}$ is an upper and lower triangular matrix defined as $\mathbf{S}_{UL} = \mathbf{EB}_{UL} + \mathbf{CQ}_{UL}$. $\mathbf{S}_D$ denotes the diagonal component of matrix $\mathbf{S}$.

The control law is then rewritten as

$$\mathbf{S}_D\boldsymbol{\Delta u}(t) = -\mathbf{F}\boldsymbol{y}(t) + \mathbf{CR}\boldsymbol{r}(t) - z^{-(k_{ij}-k_{ii})}\mathbf{S}_{UL}\boldsymbol{\Delta u}(t) \qquad (6)$$

From a realizability standpoint, it is necessary that $k_{ij} \ge k_{ii}$.

The Bezout Identity representing the closed-loop system becomes:

$$\begin{aligned}[\mathbf{B}_D\mathbf{P} + \mathbf{Q}_D\boldsymbol{\Delta}\mathbf{A}]\boldsymbol{y}(t + k_{ii}) &= \mathbf{B}_D\mathbf{R}\boldsymbol{r}(t) + \mathbf{S}_D\boldsymbol{\Delta e}(t + k_{ii}) \\ &\quad + z^{-(k_{ij}-k_{ii})}\mathbf{C}^{-1}[\mathbf{S_D B_{UL}} - \mathbf{B_D S_{UL}}]\boldsymbol{\Delta u}(t). \qquad (7)\end{aligned}$$

Then, the equation enabling the location of the closed loop poles of the system is:

$$\mathbf{B}_D\mathbf{P} + \mathbf{Q}_D\boldsymbol{\Delta}\mathbf{A} = \mathbf{T}$$

where $\mathbf{T}$ is a diagonal operator whose poles are those desired. Thus, given $\mathbf{T}$, $\mathbf{B}_D$ and $\boldsymbol{\Delta}\mathbf{A}$, matrices $\mathbf{P}$ and $\mathbf{Q}_D$ are determined from the previous equation. Uniqueness of the solution is verified if and only if $n_{bii} + n_{pi} = n_{qi} + 1 + n_{ai} = n_{\mathbf{T}}$. Then, the order of matrices $\mathbf{P}$, $\mathbf{Q}$ and $\mathbf{T}$ are chosen in the following way:

$$n_{\mathbf{P}i} = n_{ai} + 1, \quad n_{\mathbf{Q}_{Di}} = n_{bii}, \quad n_{\mathbf{T}i} = n_{ai} + n_{bii} + 1$$

From a decoupling point of view, the terms containing $\boldsymbol{\Delta u}$ in the closed loop Eq. (7) should be eliminated, since they represent an interaction. Therefore, the equation:

$$\mathbf{S}_D\mathbf{B}_{UL} - \mathbf{B}_D\mathbf{S}_{UL} = 0$$

should be satisfied. Using the decomposition of matrix $\mathbf{S}$, the previous equation can be written as:

$$\mathbf{Q}_D\mathbf{B}_{UL} - \mathbf{B}_D\mathbf{Q}_{UL} = 0 \qquad (8)$$

Since $\mathbf{B}_D$, $\mathbf{B}_{UL}$ are either known or estimated and $\mathbf{Q}_D$ is computed, $\mathbf{Q}_{UL}$ is determined so that Eq. (8) is satisfied. From an implementation point of view, $\mathbf{Q}_{UL}$ is obtained as follows:

$$\min_{\mathbf{Q}_{UL}}|\mathbf{Q}_D\mathbf{B}_{UL} - \mathbf{B}_D\mathbf{Q}_{UL}|$$

which is only an approximation of Eq. (8).

3.3. Multivariable model reference adaptive control (MMRAC)

The MMRAC technique [4] was used with the corresponding modifications and extensions given in Ref. [12]. This algorithm is difficult to adjust given the high number of parameters involved. The parameters of the controller are calculated in an algebraic form, based on the parameter identification of a model of the plant. In this case the control error goes to zero as a consequence of the identification error vanishing. When the plant has zeros outside the unit circle, it is necessary to use a compensation network that moves these zeros to the stability region. The compensation network consists in filtering the input, signal which is added to the output. Thus, the output augmented by the correction network is that which follows the reference model.

In order to algebraically compute the controller parameters, it is necessary to estimate the parameters of the model of the plant, which in this case are obtained by using the recursive least-squares method with UD factorization [14] of the covariance matrix and with a variable forgetting factor [15]. With the incremental version of the control and identification algorithms, a controller with integral action is obtained.

The following n-input n-output model of the plant is considered:

$$\mathbf{A}(z^{-1})\,\boldsymbol{y}(t) = \mathbf{B}(z^{-1})\,z^{-k}\boldsymbol{u}(t) + \boldsymbol{v}(t)$$

where $\boldsymbol{y}(t)$, $\boldsymbol{u}(t)$, $\boldsymbol{v}(t)$ are the input, output and disturbance vectors of dimension n. For the sake of simplicity, unitary delays $k=1$ are assumed. The matrix polynomials **A** and **B** are defined as:

$$\mathbf{A}(z^{-1}) = \mathbf{I}_{n\times n} + \mathbf{A}^*(z^{-1})\,z^{-1},$$
$$\mathbf{A}^*(z^{-1}) = \mathrm{diag}\left[\mathbf{A}_i^*(z^{-1})\right]; \qquad i = 1,\ldots,n$$
$$\mathbf{B}(z^{-1}) = \mathbf{B}_0 + \mathbf{B}^*(z^{-1})\,z^{-1},$$
$$\mathbf{B}_0 = \left[b_{ij0}\right]; \qquad i,j = 1,\ldots,n$$

and the perturbation vector $\boldsymbol{v}(t)$ satisfies the following property:

$$\boldsymbol{v}(t) = d + \mathbf{C}(z^{-1})\,\boldsymbol{v}'(t), \quad \lim_{t\to\infty} \boldsymbol{v}(t) = d = cte,$$
$$\lim_{t\to\infty} \boldsymbol{\Delta}\boldsymbol{v}(t) = 0$$

where $\mathbf{C}(z^{-1})$ is a monic diagonal polynomial matrix.

The structure assumed for the model is:

$$\mathbf{A}(z^{-1})\,\boldsymbol{\Delta}\boldsymbol{y}(t) = \mathbf{B}(z^{-1})\,\boldsymbol{\Delta}\boldsymbol{u}(t-1) + \mathbf{C}(z^{-1})\,\boldsymbol{\Delta}\boldsymbol{v}(t)$$

where $\boldsymbol{\Delta} = \mathbf{I} - z^{-1}$. The degrees of the polynomial elements of **A**, **B** and **C** are n_{ai}, n_{bij} and n_{ci}, respectively, with $i = 1\ldots n$ and $j = 1\ldots n$. Conversely, as **A** and **C** are diagonal, n MISO models are obtained and therefore n estimators, one for each model, are used.

The correction network is a filter that generates the signal $y_c(t)$ which is added to the real output of the plant to avoid the identified model of the plant having zeros outside the unit circle. In this case the control parameters are calculated such that the augmented output $y_a(t)$, defined in Eq. (10), follows the output of the model reference. The correction signal $y_c(t)$ is obtained in the following way:

$$\left(\mathbf{I}_{n\times n} + \mathbf{A}_c^*(z^{-1})\right)\boldsymbol{y}_c(t) = \left[\mathbf{B}_{c0} + \mathbf{B}_c^*(z^{-1})\right]\boldsymbol{\Delta}\boldsymbol{u}(t-1)$$

where

$$\mathbf{A}_c^*(z^{-1}) = \mathrm{diag}\left[\mathbf{A}_{ci}^*(z^{-1})\right]; \qquad i = 1,\ldots,n$$
$$1 + \mathbf{A}_{ci}^*(z^{-1})\,z^{-1} = 0, \qquad \text{for } |z| > 1 \tag{9}$$
$$\mathbf{B}_{c0} = \left[b_{cij0}\right].$$

The augmented output of the plant is defined as:

$$\boldsymbol{y}_a(t) = \mathbf{y}(t) + \boldsymbol{y}_c(t) \tag{10}$$

The parameters of the correction network should be calculated such that the zeros of the augmented plant be inside the unit circle, meaning that, they must satisfy:

$$\det\left[\mathbf{A}(z^{-1})\left(\mathbf{B}_{c0} + \mathbf{B}_c^*(z^{-1})\,z^{-1}\right)\boldsymbol{\Delta} + \left(\mathbf{I} + \mathbf{A}_c^*(z^{-1})\,z^{-1}\right)\mathbf{B}(z^{-1})\right] \neq 0 \qquad \forall\,|z| \geq 1$$

Let us consider the reference model

$$\left(\mathbf{I}_{n\times n} + \mathrm{diag}[\mathbf{A}_{mi}^*]\,z^{-1}\right)\boldsymbol{y}_m(t) = \mathbf{B}_m\boldsymbol{r}(t-1)$$

where $\boldsymbol{r}(t) \in \Re^n$ is the reference vector and $\boldsymbol{y}_m(t) \in \Re^n$ is the output vector of the reference model.

The augmented error signal is defined as:

$$\boldsymbol{e}(t) = \boldsymbol{y}_m(t) - \boldsymbol{y}_a(t). \tag{11}$$

Then the dynamic behavior of the error signal can be obtained by replacing $\boldsymbol{y}_a(t)$ and $\boldsymbol{y}_m(t)$ in Eq. (11), which can be written as:

$$\mathbf{A}_m(z^{-1})\,\boldsymbol{e}(t) = z^{-1}\Big[\left(\mathbf{A}_c^*(z^{-1}) - \mathbf{A}_m^*(z^{-1})\right)\boldsymbol{y}_c(t) + \left(\mathbf{A}^*(z^{-1})\,\boldsymbol{\Delta} - \mathbf{A}_m^*(z^{-1})\right)\boldsymbol{y}(t) + \mathbf{B}_m(z^{-1})\,\boldsymbol{r}(t) - \left(\mathbf{B}(z^{-1}) + \mathbf{B}_c(z^{-1})\right)\boldsymbol{\Delta}\boldsymbol{u}(t)\Big]$$

Then, making $\boldsymbol{e}(t) = 0$ the following control law for this algorithm is obtained:

$$\left(\mathbf{B}(z^{-1}) + \mathbf{B}_c(z^{-1})\right)\boldsymbol{\Delta}\boldsymbol{u}(t) = \mathbf{B}_m(z^{-1})\,\boldsymbol{r}(t) + \left(\mathbf{A}_c^*(z^{-1}) - \mathbf{A}_m^*(z^{-1})\right)\boldsymbol{y}_c(t) + \left(\mathbf{A}^*(z^{-1})\,\boldsymbol{\Delta} - \mathbf{A}_m^*(z^{-1})\right)\boldsymbol{y}(t) \tag{12}$$

3.4. Multivariable direct nyquist array control (MDNAC)

Amongst the conventional multivariable control techniques one of the most used is the Direct Nyquist Array (DNA) [1,10,13,18,38], consisting of an interactive design method in the frequency domain. The objective is to reduce coupling between different loops in the process, and later applying SISO control techniques and using direct Nyquist diagrams. The method requires a PID type diagonal controller, that will be designed by the Internal Model Control (IMC) method [19,20].

Fig. 2 illustrates the structure of a multivariable control system. $\mathbf{C}(s)$ is the multivariable controller, $\mathbf{K}(s)$ is the compensator to reduce the coupling effects, $\mathbf{G}(s)$ represents the plant and $\mathbf{F}(s)$ is a feedback matrix. All the matrices have the same dimension $(m \times m)$. $\mathbf{C}(s)$ is a diagonal matrix whose elements are PI controllers. $\mathbf{K}(s)$ can be a static or dynamic compensator and $\mathbf{F}(s)$ corresponds to a constant diagonal matrix called a feedback matrix gain.

One of the central concepts in the design via DNA is diagonal dominance, which is a measure of the reduction of the interaction between loops. It is desired that the output associated with the diagonal transfer function dominates the net effects associated with all the other transfer

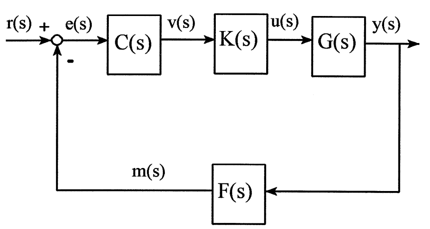

Fig. 2. General structure of a multivariable control system.

functions outside the diagonal, and satisfying this for all rows or columns.

Let us consider the matrix transfer function of a feedback system, as shown in Fig. 2:

$$\mathbf{H}(s) = \left[\mathbf{I}_{\mathrm{m}} + \mathbf{Q}(s)\mathbf{F}(s)\right]^{-1}\mathbf{Q}(s)$$

where $\mathbf{Q}(s)$ is the forward path matrix transfer function defined as:

$$\mathbf{Q}(s) = \mathbf{G}(s)\mathbf{K}(s)\mathbf{C}(s).$$

In the design process via DNA, the objective is to obtain diagonal dominance for the matrices $\mathbf{Q}(s)$ and $\mathbf{H}(s)$. A matrix $\mathbf{D}(s)$ is said to be diagonal dominant for columns, if

$$|d_{jj}(s)| > \sum_{i=1,\, i\neq j}^{m} |d_{ij}(s)| \qquad j = 1,\dots,m$$

The diagonal dominance can be easily established through graphs using matrix $\mathbf{D}$ and drawing the elements d_{ii} and sum of the outer diagonal terms of row i (dominance by rows) or i column (dominance by columns), in the complex plane. When those circles are drawn for a frequency range, an envelope circle is formed, called Gershgorin bands.

For diagonal dominance of columns, graphic verification consists of:

(i) To plot in the complex plane q_{ii}, i.e., the frequency response of the ith diagonal element of $\mathbf{Q}$.

(ii) To evaluate

$$|d_{ii}(jw)| = \sum_{k=1,\, k\neq i}^{m} |q_{ki}(jw)|$$

(iii) Placed on q_{ii} trace a circumference of radius $d_{ii}(jw)$.

(iv) To carry out stages (i) to (iii) for the desired range of frequencies. The envelope of circumferences determines a band denominated ith band of Gershgorin.

(v) To repeat the stages (i) to (iv) for each column of $\mathbf{Q}$.

$\mathbf{Q}$ is diagonal dominant for columns if and only if no Gershgorin band encircles or contains the origin. The distance from the center of the circumference to the origin should be greater than its radius. It is not possible to achieve dominance by using a diagonal compensator and it is certainly not possible to modify the dominance of a DNA column, or the dominance for the rows of an INA using diagonal precompensators. A method is needed to automatically generate compensators comprising a more general structure. This may be accomplished by selecting a measure of the dominance, a structure for the compensator and then optimizing the measure of dominance for all compensators containing such a structure.

Pseudodiagonalization [22] will be used for such a purpose (although the term is often reserved for the scheme proposed by Hawkins [21]). In his work, Hawkins used the DNA, but the INA can also be used.

If we have plant $\mathbf{G}(s)$ and a constant compensator $\mathbf{K}$, with $\mathbf{Q}(s) = \mathbf{G}(s)\mathbf{K}$, then the elements of $\mathbf{Q}(s)$ are given by:

$$q_{ij}(jw) = g_i^{\mathrm{T}}(jw)\,k_j$$

where $g_i^{\mathrm{T}}(s)$ denotes the ith row of $\mathbf{G}(s)$ and k_j denotes the jth column of $\mathbf{K}$.

Hawkins proposed minimizing

$$J_j = \sum_{k=1}^{N} p_k \sum_{i\neq j} |q_{ij}(jw_k)|^2 = \sum_{k=1}^{N} p_k \sum_{i\neq j} |g_i^{\mathrm{T}}(jw_k)\,k_j|^2$$

constrained to $\|k_j\| = 1$. $\{p_k\}$ for $k = 1,2,\dots N$, is a set of weighing coefficients and the solution using the Lagrange multipliers can be easily obtained. Replacing the criteria by:

$$J_j = -\sum_{k=1}^{N} p_k \left\{ \sum_{i\neq j} |g_i^{\mathrm{T}}(jw_k)\,k_j|^2 \right\} \Big/ \sum_{k=1}^{N} p_k |g_j^{\mathrm{T}}(jw_k)\,k_j|^2 \qquad (13)$$

which is a better measure of the dominance column, and has the advantage in that it can be minimized without placing constraints on $\mathbf{K}$. This result has been extended to dynamic compensators [1] of the type

$$\mathbf{K}(s) = \left[\boldsymbol{k}_1(s),\dots,\boldsymbol{k}_m(s)\right]$$

where each column has the form

$$\boldsymbol{k}_j(s) = \boldsymbol{k}_{0j} + \cdots + \boldsymbol{k}_{\beta j}\, s^{\beta}, \qquad j = 1,2,\dots,m$$

and each $\boldsymbol{k}_{ij}$ is a column vector; $\beta \in \mathbb{Z}$. In this case:

$$q_{ij}(jw) = g_i^{\mathrm{T}}(jw)\,k_j(jw)$$

is replaced by

$$q_{ij}(jw) = \boldsymbol{\gamma}_i^{\mathrm{T}}(jw)\,\boldsymbol{\eta}_j$$

where $\boldsymbol{\gamma}_i^{\mathrm{T}}(jw)$ is the row vector

$$\boldsymbol{\gamma}_i^{\mathrm{T}}(jw) = \left[g_i^{\mathrm{T}}(jw),\, jwg_i^{\mathrm{T}}(jw),\,\dots,\,(jw)^{\beta} g_i^{\mathrm{T}}(jw)\right]$$

and $\boldsymbol{\eta}_j$ is the column vector

$$\boldsymbol{\eta}_j = \left[k_{0j},\dots,k_{\beta j}^{\mathrm{T}}\right]^{\mathrm{T}}$$

In order to maximize the dominance of columns [1], the cost function is minimized such that in this case takes the form

$$J_j = -\sum_{k} p_k \left\{ \sum_{i\neq j} |\boldsymbol{\gamma}_i^{\mathrm{T}}(jw_k)\,\boldsymbol{\eta}_j|^2 \right\} \Big/ \sum_{k} p_k |\boldsymbol{\gamma}_j^{\mathrm{T}}(jw_k)\,\boldsymbol{\eta}_j|^2$$

If column dominance for $\mathbf{G}(s)\,\mathbf{K}(s)$ is achieved, it is not lost by scaling the columns of $\mathbf{K}(s)$. A realizable compensator is obtained through dividing $\boldsymbol{k}_j(s)$ by a polynomial of degree β or greater. The chosen polynomial has have stable roots, with pole locations so as to obtain the desired loop compensation.

The pseudodiagonalization can be applied to either the INA or to the DNA methods. In the INA method, the inverse of the desired precompensator should be realizable.

MATLAB's MFD Toolbox was mainly used in the analysis and design of precompensators in the frequency domain applying the DNA. This software comes with the tools to design a multivariable control system in the frequency domain [23–26].

The function damp was used in order to determine the frequency range. The Nyquist diagram and the circles of Gershgorin were plotted by using *plotnyq* and *fcgersh*, respectively. For the analysis of the dominance, in dB, the function *fcdom* was employed. In the design of a dynamic precompensator the function *fpseudo*, was used, which employs the Pseudodiagonalization method.

3.5. Multivariable sequential loop closing control (MSLCC)

A simpler way of designing multivariable controllers is to ignore the multivariable nature of the process. The idea is to design the controller parameters sequentially, as long as the loops are being closed, while considering the loops closed in the adjustment of the parameters [1,18]. A SISO controller is designed for a pair of input–output variables. When this design is successful, another SISO type controller is designed for another pair of input–output variables, and so on. This procedure is often adopted when the structure of the controller is restricted to being diagonal (matrix transfer function of the controller is diagonal). It has the further advantage in that it can be implemented closing one loop at a time, since the procedure assures that the system remains stable at each step, which is of great importance in the control process. If a totally coupled controller is used, all the loops should be closed simultaneously, although this does not ensure system stability.

4. Practical aspects of the industrial implementation

In the implementation of the control strategies upon the grinding plant a series of practical aspects were considered, which are described below.

4.1. Data acquisition system

All the signals coming from the sensors of the grinding and flotation plant are collected in the DCS (Distributed Control System DCI-4000 Fisher and Porter) available at present in the CODELCO-Andina plant, as shown in Fig. 3. This system is based on hierarchical concepts, organized in functional and geographical groups. All the signals received by the DCI 4000 are saved in a data-base. Also, control strategies can be programmed on it and it has two displays directly connected to the grinding console. The DCS is connected to a VAX station through a Data Highway network. A third display on the flotation console is connected to the DCS through the Data Highway network. The VAX station, working with the VMS operating system, supports the control software, SCAUT, and has a data base with all the variables configured in the DCS. It is sufficient to change the value of the associated variable on the VAX data base in order to manipulate any of the actuators (this means is used to implement and test the multivariable control strategies from a PC).

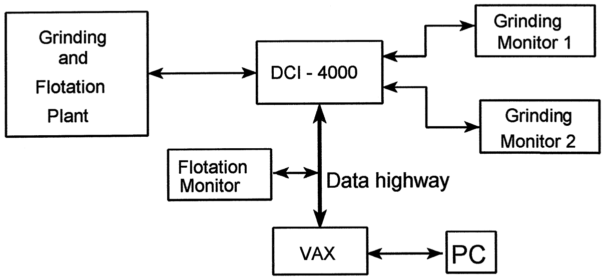

Fig. 3. Data acquisition system.

Using CSPC software, a personal computer (PC) was connected through its serial port to one of the VAX station's ports. On the PC, the control software containing the multivariable strategy, programmed in Turbo Pascal, was executed along with the read/write routines of the desired variables on the VAX station's data base.

4.2. Communication errors

Some reading and/or writing errors can occur on the data base of the VAX station during the control process. These errors can modify the parameter estimates substantially and may lead to a loss of control. If a communications error is detected in any variable, three further attempts are made. If the read error persists, the last correct reading is taken.

4.3. Sampling period

After several trial runs and information from previous simulations of the control strategies, the sampling period chosen was equal to 15 s which is 1/10 of the time constant of the relationship between the percentage of solids–sump water flow, 1/9 of the time constant of the percentage of solid–pump speed, 1/9 of the time constant of the sump level–sump water flow, and 1/4 of the time constant of the sump level–pump speed.

4.4. Filtering signals

Digital Butterworth filters were designed for the percentage of solids, the sump level, the sump water flow and the pump speed. Their cut frequencies are: 0.00371, 0.00371, 0.00593 and 0.00698 Hz, respectively. The filters are of first order to avoid phase distortion problems. In order to avoid filter interference on the control process, all input and output signals were filtered by the same filter [5], using the one with the greatest cut frequency [12].

4.5. Exciting signals

It is necessary to add excitation signals to the normal inputs of the plant in order to obtain good parameter estimates. In a multivariable system a single binary random sequence is used, to which a time delay is added as this sequence is applied to each different input, to avoid a correlation between the excitation signals added to each of the inputs. This time-delay should be larger than the sum of the largest time-delays of the system and the largest order of the model. The amplitude of the binary excitation signal is proportional to the trace of the covariance matrix when a given threshold has been reached, otherwise the amplitude is zero.

4.6. Numerical problems

The UD factorization algorithm [14] was used in the recursive computation of the covariance matrix to avoid numerical uncertainties. As 32-bit floating point variables are used, rounding problems can become significant on considering between 5000 and 10 000 samples from the starting point of the estimator [16]. However, all of the signals used in the control and identification algorithms are normalized between 0 and 1 with respect to their normal range of operation thus guaranteeing the real contribution of each variable to the estimated model.

5. Plant implementation of the multivariable techniques

Numerous simulations in a specially developed simulator [17] were performed prior to in-plant implementation, which are reported in Ref. [35].

Several experimental tests were carried out on Section C of the grinding plant of CODELCO Chile-Andina Division, described in Fig. 1, using the implementation detailed in Section 4.

In general, the tests were performed under current plant operating conditions. This is why it was impossible to perform all the planned reference changes and why in some cases it is necessary to accept the changes that the operation of the plant imposes, most of which are made to avoid mill overload.

As mentioned in Section 4, the sampling period chosen in the multivariable strategies was as $T_s = 15$ s. As far the process of signal conditioning is concerned, the percentage of solids, sump level, sump water flow and pump speed, and the filters designed in Section 4 were used. These variables are also normalized, as described in Section 4, and to this end Table 1 shows the ranges with respect to which the variables have been normalized.

A protection system against communications errors, as described in Section 4, has been included in the multivariable algorithms.

Table 1
Values respect to which the normalization variable was performed and used in the multivariable strategies implemented in plant

	Percentage of solids [%]	Sump level [%]	Valve opening [%]	Pump speed [%]
Minimum value	65	10	10	15
Maximum value	80	90	80	90

All of the control variables were limited to acceptable values established by the normal operation of the plant in order to secure correct actuator operation.

5.1. Multivariable extended horizon adaptive control

Preliminary results regarding the application of this method to grinding plants can be found in Ref. [39], for both simulations, as well as on plant experiments.

Following numerous modeling tests on the plant it was determined that the percentage of solids and sump level responses are mainly of first order and consequently that the best observability indexes for the model of the plant described in Section 3.1 are $q_i = 1$ for $i = 1,2$. Thus, eight parameters have to be estimated and according to the formulation of the state space, shown in Section 3.1, the matrices **A**, **B** and **C** are of 2×2. The most convenient values for the delays turned out to be $k = 2$ sampling periods, i.e., $k = 30$ s since the sampling period was chosen as 15 s.

During the course of preliminary testing it was determined that the best pair of values for the control horizons were $T_1 = 10$ and $T_2 = 10$ sampling periods (i.e., $T_1 = T_2 = 150$ s). It was also found that the best value for the nominal memory of the estimators is $S_0 = 0.002$.

The application of this technique upon the grinding plant is described in Table 2 and is performed on ball mill 9 of Section C.

The conditions under which the test is carried out are fairly critical, because although the mineral feed to the bar mill is relatively smooth and constant, ball mill No. 8 stopped and started on several occasions during the test.

The effects of stopping one ball mill in Section C are striking. Every time ball mill No. 8 stops, the load being processed is distributed transitorily to ball mills No. 7 and 9 from the halt until the feed tonnage to Section C is decreased, as every time a ball mill stops the operator diminishes the feed tonnage to the section. The reverse happens when the ball mill starts again, when part of the load is removed from ball mills No. 7 and 9. It is also worth mentioning that the dynamics regarding increasing the feed tonnage are slower than those for decreasing it, which means that the controller faces different conditions in the two situations.

In regard to the overload phenomenon in the ball mills, two of them occurred in closed loop during the experi-

Table 2
Experiments performed on the grinding plant of CODELCO-Andina

Time interval [min]	Reference of percentage of solids [%]	Reference of sump level [%]
44–47	71	42
47–68	71	50
68–87	73	50
87–102	73	40
102–114	71	40
114–120	70	40
120–133	73	40
133–139	72	40
139–141	72	35
141–149	70	35
149–157	69	35
157–163	69	45
163–174	71	45
174–177	69	45
177–185	71	45
185–193	71	35
193–200	73	35

MEHA controller.

ment, one at approximately 60 min and the other at 114 min.

The results of the test are shown in Figs. 4 and 5. In Fig. 5, the sump water flow and the opening of the valve are plotted for the sake of comparison, because during the experiment systematic water pressure variations occur.

The following is a chronological account of the experiment. Persistent excitation, in open loop, is applied at the start of the test for 43 min taking into account all of the operational constraints on the input variables. Later, at $t = 44$ min the control loop is closed, while bearing in mind all of the practical considerations mentioned in Section 4.

In Fig. 4, at 47 min, it is observed that when the reference level is raised from 40% to 50%, there are almost no coupling effects in the percentage of solids. The behavior of the manipulated variables is plotted in Fig. 5. Both variables present changes of the same magnitude despite the weak interaction between the percentage of solids and the pump speed.

At $t = 60$ min, ball mill No. 8 is stopped and the entire load is transitorily processed by ball mill Nos. 7 and 9. The effect is clearly appreciated in Fig. 4, which shows the percentage of solids and the sump level deviating from their reference values. This is the first large deviation of the sump level with respect to its 50% reference. Since the amount of pulp sent toward Line No. 9 has increased, and since it is desirable to maintain the percentage of solids as close as possible to its reference (71%), the multivariable controller increases the valve opening to values near 80%. However, Fig. 5 shows that the corresponding water flow does not rise proportionally, and remains saturated at a value close to 4000 LPM. At this point the feed tonnage to

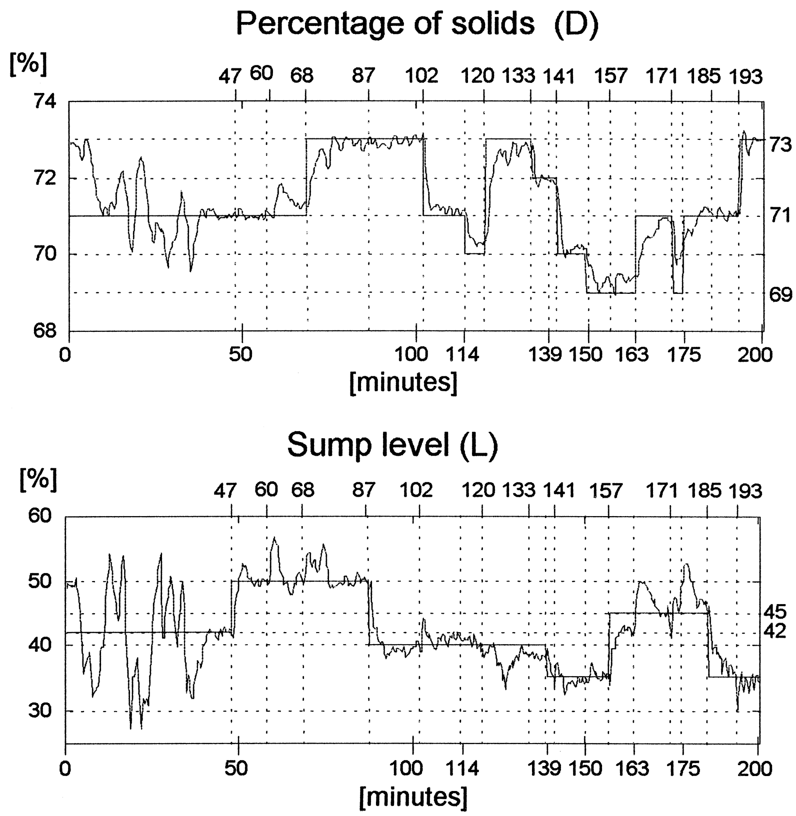

Fig. 4. Controlled variables for the in-plant implementation of the MEHAC.

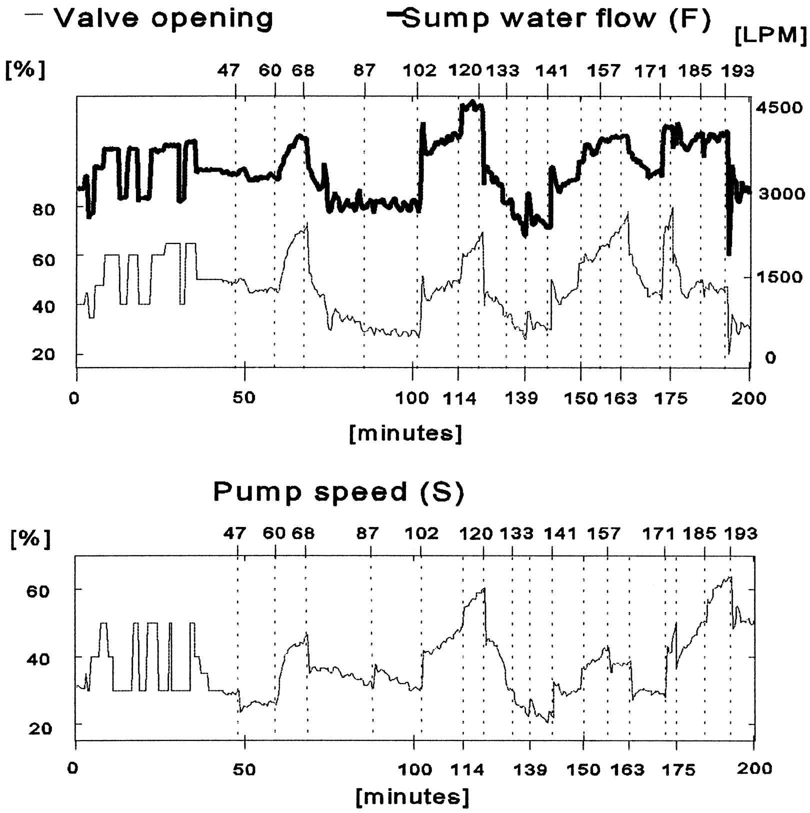

Fig. 5. Manipulated variables for the in-plant implementation of the MEHAC.

the bar mill is reduced by the operator from 515 TPH to 410 TPH.

There are significant variations in the estimated parameters given the stoppage of ball mill No. 8 and saturation of the water flow.

The stoppage of ball mill No. 8 pushes ball mill No. 9 toward a state of overload. One way of addressing this is by increasing the percentage of solids reference. This reference is therefore changed at 68 min from 71% to 73%. The amount of water then entering the sump diminishes, as can be seen in Fig. 5, and thus ball mill No. 9 maintains its electric power within acceptable values. At this point there are also variations in the water pressure and the changes in the valve opening are not proportional to the water flow. The second large deviation of the sump level with respect to its 50% reference is observed in Fig. 4, when the change in the reference of percentage of solids is produced at 68 min. This is due to the combined effect of variations in the water pressure and coupling, which is more severe in this case because the accuracy of the estimated parameters is impaired by the stoppage of ball mill No. 8 at 60 min.

At $t = 87$ min, the level reference is decreased from of 50% to 40% and there is practically no coupling in the percentage of solids. It can be seen in Fig. 5 that only the pump speed changes, which is partly due to the fact that parameters have already been adjusted after the stoppage of ball mill No. 8 and to the low degree of coupling between the pump speed and the percentage of solids

At $t = 102$ min, the percentage of solids reference is changed from 73% to 72%, and a small coupling in the level can be discerned in Fig. 4. The percentage of solids reference is decreased from 71% to 70% at 114 min, as appreciated in Fig. 4, and a coupling in the level is barely noticeable. The valve opening continues to increase at $t = 120$ min, however the water flow is saturated, which is appreciable from Fig. 5 and occurs due to insufficient water pressure in the piping. Despite the water flow being saturated, the amount of water entering the sump is sufficient to bring on the overload of ball mill No. 9. Under these circumstances the percentage of solids cannot reach the 70% reference, so at 120 min, it is necessary to increase it to 73% as shown in Fig. 5. This action diminishes the amount of water to the sump and avoids the ball mill from overloading.

At 123 min, ball mill No. 8 starts up again and the feed tonnage is increased abruptly by the operator from 410 TPH to 475 TPH and then on gradually up to 500 TPH over a period of 20 min. With respect to the identification process, this action causes significant variations in all of the estimated parameters. When ball mill No. 8 begins to work again the operator reduces the load from ball mill Nos. 7 and 9 until the overall effect of an increase in tonnage is felt in the system. This effect can be appreciated in Fig. 4 through the decrease in the sump level with respect to its reference. Also during this change, large variations in all the estimated parameters are observed regarding the identification process.

At 133 min when the reference of percentage of solids is changed from 73% to 72% and at 141 min from 72% to 70%, it is appreciated in Fig. 5 that proportionality exists between the valve opening and the water flow, although the level is still influenced by the effect of ball mill No. 8 restarting. Also in Fig. 4, it is seen that at $t = 139$ min, the sump level reference is changed from 40% to 35%, which is easy to control, because with the start of ball mill No. 8 at 123 min, the level has a tendency to decrease. No coupling is detected in the percentage of solids at this point.

The reference of percentage of solids is decreased at 149 min from 70% to 69%, with Fig. 5 showing that the valve begins to open again while at approximately 160 min the water flow is saturated since there is insufficient pressure in the piping. Therefore, at 163 min, the reference of the percentage of solids is increased from 69% to 71%, as depicted in Fig. 4. The first large deviation of the sump level, with respect to its reference of 45%, is due to the coupling effect and to the degradation of the estimated parameters upon saturation of the water flow. At 157 min, the level reference is changed from 35% to 45% and Fig. 4 indicates almost no coupling effects in the percentage of solids despite the sump water flow being saturated.

At 171 min when the reference of the percentage of solids is changed from of 71% to 69%, in Fig. 5 it can be seen that the valve reaches its upper limit of 80% when the water flow had been saturated long before. For this reason at $t = 177$ min, it is necessary to raise the reference of the percentage of solids from 69% to 71%. At 175 min, ball mill No. 8 stopped again and the tonnage is reduced by the operator from 500 TPH to 410 TPH. Fig. 4 shows the second large deviation, at approximately 180 min, of the level from its reference of 45% which is due to the stoppage of ball mill No. 8 and to the almost complete saturation of the sump water flow incurring large variations in all the estimated parameters.

When the sump level reference is changed from 45% to 35% at 185 min, from Fig. 4 it can be appreciated that this change does not affect the percentage of solids. Finally, at 193 min the reference of the percentage of solids is increased from 71% to 73% which does disturb the sump level slightly. The test concludes at approximately 200 min.

5.2. Multivariable pole placement adaptive control (MPPAC)

This technique has been applied previously for which preliminary results are presented in Refs. [40,41] covering both simulations and applications in grinding plants.

Following numerous modeling tests and analysis of the phenomenological knowledge of the grinding plant it was determined that the system is a predominantly first order one with time-delays. According to the structure of the model of the plant then, as described in Section 3.2, the polynomial order of $\mathbf{A}_i(z^{-1})$ are chosen as $n_{ai} = 1$ for $i = 1,2$. The possibility of finding pole zero cancellations was diminished by choosing unitary time-delays and thus, the probability of obtaining a solution for the Bezout Identity was increased. The most appropriate values for the order of the remaining polynomials are: $n_{bij} = 2$ and $n_{ci} = 1$ for $i = 1,2$ and $j = 1,2$. Finally, the most suitable values regarding the time-delays were: $k_{11} = 2$, $k_{12} = 2$, $k_{21} = 1$ and $k_{22} = 1$ sampling periods, with a sampling period of 15 s.

The closed loop poles were located at 0.7 with a multiplicity of two for both loops in order to get a better representation of the plant's dynamics and improved closed loop system response. The best values for the nominal memories of the estimators were established as $S_{01} = 0.003$ and $S_{02} = 0.002$ for the models of the percentage of solids and level, respectively. The value of D_0 (the threshold in determining the existence of common factors in the Bezout Identity) is chosen as 0.0001.

The control technique was applied to the grinding plant according to changes detailed in Table 3 and which is carried out on ball mill No. 8.

Test conditions are taken as normal, in which ball mill No. 9 is out of service during the whole test while ball mill No. 7 operates continuously. The mineral feeding the bar mill is hard until $t = 129$ min when the hardness diminishes notably. The feed tonnage to the bar mill remains constant at 378 TPH. The water pressure, on the other hand, remains constant during the whole test except for a sudden surge at 175 min.

Four situations of overload were recorded in the ball mill; two in open loop (during the excitation period) and two in closed loop.

Table 3
Description of the experiment performed at the CODELCO-Andina grinding plant

Time interval [min]	Reference of percentage of solids [%]	Reference of sump level [%]
0–76	75	40
76–85	73	40
85–87	73	30
87–102	75	40
102–119	77	40
119–129	77	30
129–134	75	30
134–152	72	30
152–161	72	40
161–189	74	40
189–205	74	30

MPPAC.

The results of the plant implementation of this control technique are shown in Figs. 6 and 7. The experiment is now described chronologically.

The test begins with the application of persistent excitation in open loop for 70 min, as shown in Fig. 6, while considering all operational constraints. At $t = 71$ min the control loop is closed with the reference of the percentage of solids at 75% and that of the level at 40%. During the period of excitation the ball mill twice enters in a state of overload; at $t = 8$ min and at $t = 44$ min.

At 76 min, when the reference of the percentage of solids is reduced form of 75% to 73%, Fig. 6 shows no coupling in the level. Also, slight variations are observed in the identification process in all the estimated parameters.

A little later, at $t = 85$ min, when the reference of the sump level is decreased from 40% to 30%, the ball mill begins to enter a state of overload, because the electric power falls to values near 1180 kW, therefore making it very difficult to decrease the level, as shown in Fig. 6. In Fig. 7 one can see how the pump speed increases while Fig. 6 shows that the level does not significantly decrease. In order to alleviate the ball mill then, at 87 min both references are increased; the percentage of solids from 73% to 75% and the level from 30% to 40%. Significant variations in all the estimated parameters are observed during these changes as far as the identification process is concerned.

After 102 min have elapsed from the beginning of the experiment, the reference of the percentage of solids is increased from 75% to 77% and that there are almost no coupling effects on the level nor overshoot in the percentage of solids, as is observable in Fig. 6. Also, at this point, the electric power begins to increase and the ball mill begins to recover.

At $t = 119$ min, when the reference of level is decreased from 40% to 30%, Fig. 6 shows that there is almost no coupling in the percentage of solids and that the level response exhibits little overshoot.

At 129 min, the reference of the percentage of solids is changed from 77% to 75%, and also, at this point, the decrease in the hardness of the mineral feeding the bar mill begins to be felt by the system. This is detected by an increase in the electric power (as now the grinding is much finer and the classification at the hydrocyclone improves), thus the volumetric flow of pulp to hydrocyclones diminishes and so does the circulating load. In this situation, the sump level tends to decrease and, in order to maintain it at its reference value the multivariable control has to decrease the pump speed to values approaching 13%, as shown in Fig. 7. This occur at 129 min and at 134 min. From the identification standpoint, large variations in all the estimated parameters are observed at these times.

At $t = 134$ min, when the reference of the percentage of solids is decreased from 75% to 72%, a small coupling effect on the level is noticed in Fig. 6, that is partly due to

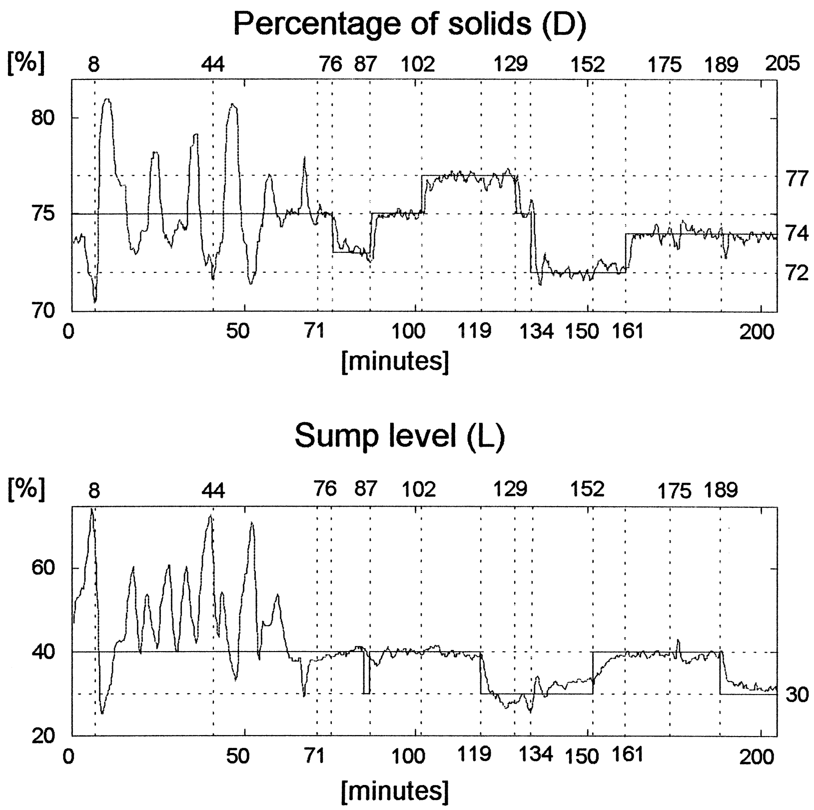

Fig. 6. Controlled variables for the implementation in plant of the MPPAC.

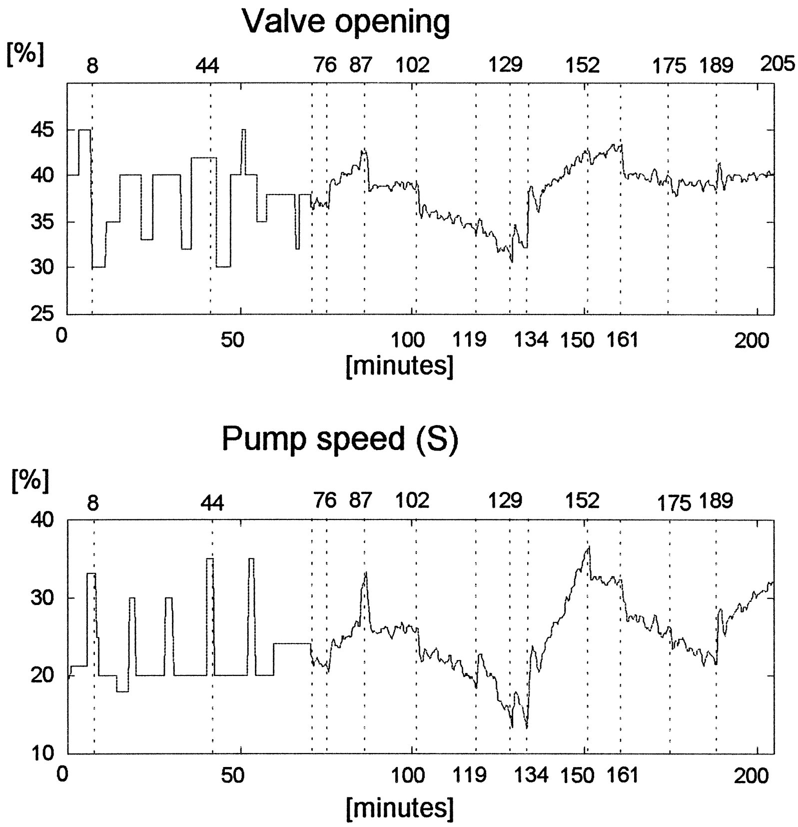

Fig. 7. Manipulated variables for the in-plant implementation of the MPPAC.

the adjustments in parameter resulting from the changes in mineral hardness.

At 152 min, when the reference of the level is changed from 30% to 40%, a small coupling on the percentage of solids is seen in Fig. 6, since the estimated parameters still vary fairly significantly.

Since the reference of the percentage of solids cannot be kept at a low value for long, and since a large amount of water goes to the sump easily generating a state of overload, it is necessary to increase the reference from 72% to 74% (at 161 min). It is clearly observed in Fig. 6 that there is no coupling on the level. Also, the estimated parameters have already reached steady values by this point.

At $t = 175$ min, there is a sudden change in the water pressure, at first causing a positive peak on the sump water flow and then a negative one. This disturbance affects the percentage of solids and the level, as shown in Fig. 6. At that instant, some estimated parameters in the identification process exhibit significant variations among both models: the percentage of solids and level. Finally, at $t = 189$ min, the level reference is decreased from 40% to 30%, and a small coupling in the percentage of solids is observed in Fig. 6, that is partly due to the fact that the estimated parameters were deteriorated by the disturbance in the water flow. The test ends at approximately 200 min.

5.3. *Multivariable model reference adaptive control (MMRAC)*

Some previous results relative to applications of this algorithm are shown in Ref. [42] for both simulations and in plant implementation.

After using phenomenological knowledge and data obtained from modeling, it was determined that the most appropriate degrees for the polynomials of the model of the plant presented in Section 3.3 were $n_{ai} = 1$, $n_{bij} = 2$ and $n_{ci} = 1$ for $i = 1,2$ and $j = 1,2$. Similarly it was determined that the most suitable values for the time-delays were $k_{ij} = 2$ for $i = 1,2$ and $j = 1,2$.

It was also determined that the most convenient reference model has the following form:

$$\boldsymbol{y}_{mi}(t) = \boldsymbol{r}_i(t) \qquad \text{for } i = 1,2$$

After a series of preliminary tests it was found that the best correction network has the following form:

$$\begin{aligned} \boldsymbol{y}_{c1}(t) &= 0.1\boldsymbol{y}_{c1}(t-1) + 0.1\boldsymbol{y}_{c1}(t-2) - 3\boldsymbol{\Delta}_{u1}(t-2) \\ &\quad - 0.1\boldsymbol{\Delta}_{u2}(t-2) \\ \boldsymbol{y}_{c2}(t) &= -0.2\boldsymbol{y}_{c2}(t-1) + 0.1\boldsymbol{y}_{c2}(t-2) \\ &\quad - 0.1\Delta_{u1}(t-2) - 10\Delta_{u2}(t-2) \end{aligned}$$

The preliminary tests also allowed the determination of the best values for the nominal memories of the estimators, which turned out to be $S_{01} = 0.003$ and $S_{02} = 0.002$.

Table 4
Experiment carried out at the CODELCO-Andina grinding plant with the MMRAC

Time interval [min]	Reference of percentage of solids [%]	Reference of sump level [%]
0–49	74	47
49–64	72	47
64–80	72	68
80–96	74	60
96–111	74	40
111–124	72	40

The application of this technique to the grinding plant is described in Table 4 and was carried out on ball mill No.9.

The conditions under which the experiment was carried out are normal. All three Section C ball mills (Nos. 7, 8 and 9) were working continuously. During the experiment the feed tonnage remains constant at 482 TPH and the condition of the mineral remains stable, in medium hard state. The sump water pressure remains approximately constant over the course of the whole experiment at an intermediate value and despite no variations in pressure, between $t = 72$ min and $t = 80$ min the valve opening was such that the sump water flow remains saturated.

Five overload states occurred during the test in the ball mill: two in open loop (during the initial identification period) and three in closed loop while the controller was acting. Next, the experiment is described in chronological order and plotted in Figs. 8 and 9.

At the start of the test, persistent excitation is applied in open loop for 19 min while taking into account all practical considerations. At $t = 5$ min and $t = 11$ min states of overload in the ball mill are detected, in which the electric power descends to values of approximately 1180 kW.

At 21 min, the control loop is closed with a correction network obtained from tests on a simulator of the grinding plant, but oscillatory behavior of the system was observed, as shown in Fig. 8. The network is adjusted on line until $t = 38$ min where a correction network providing good system behavior is found. At this point, the values of the references remain constant at 74% and 47% for the percentage of solids and level, respectively.

At 49 min, when the percentage of solids reference is reduced from 74% to 72%,a large coupling affecting on the level can be seen in Fig. 8. The estimated parameters in the identification process remain almost unaffected during this change.

At $t = 64$ min the level reference is changed from 47% to 60% and Fig. 8 identifies slight coupling in the percentage of solids and a large overshoot in the level. Also, variations in all the on line estimated parameters are detected here. Fig. 9 shows that due to the coupling in the percentage of solids at 64 min, the multivariable controller begins to open the valve to deliver more water to the sump and at approximately $t = 72$ min the sump water flow

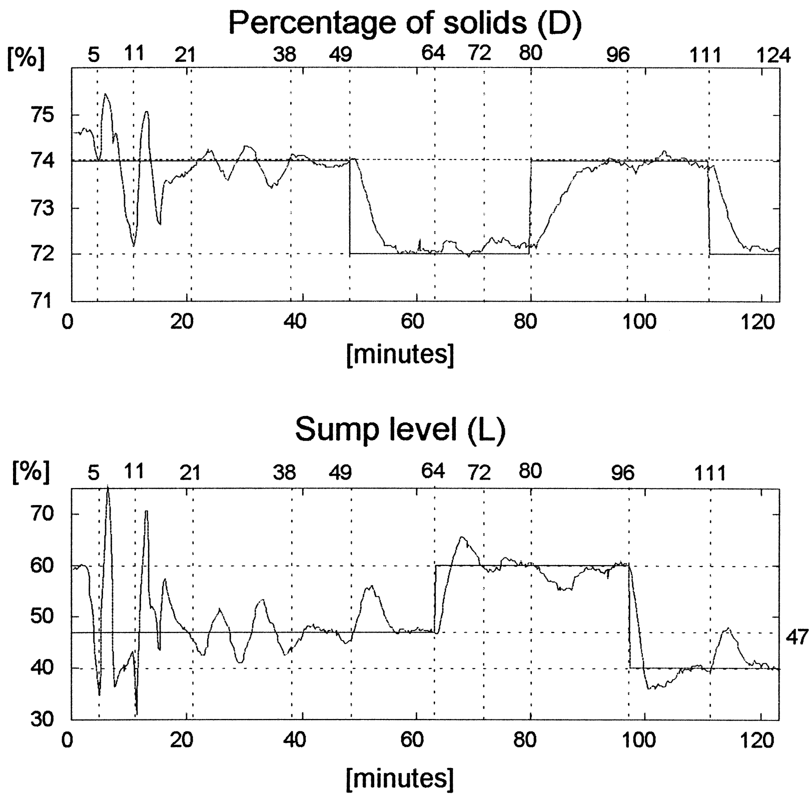

Fig. 8. Controlled variables for the in-plant implementation of the MMRAC.

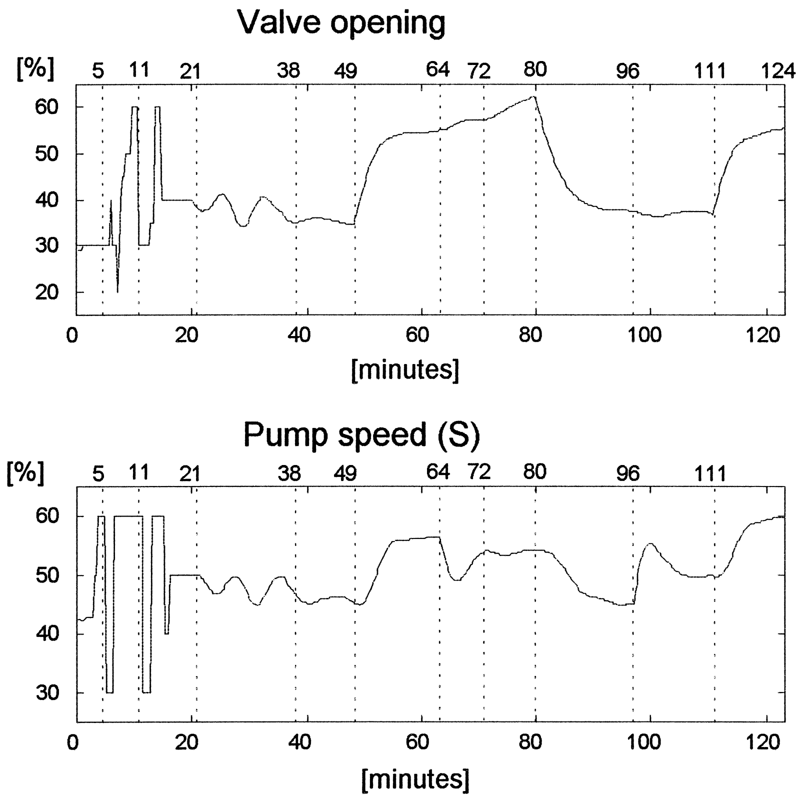

Fig. 9. Manipulated variables for the in-plant implementation of the MMRAC.

becomes saturated. For this reason, the percentage of solids remains at its reference value as shown in Fig. 8.

The ball mill begins to overload just before 80 min, since the reference of percentage of solids has remained at a low value (72%) over a long period, with it being necessary to increase it in order to recover the mill. Hence, at 80 min the reference of percentage of solids is changed from 72% to 74%. The effect of the coupling on the level is seen in Figs. 8 and 9 shows that the valve opening is diminished to increase the percentage of solids and, at the same time, the pump speed is decreased to avoid the level going down. This last action is not efficient however, and causes the coupling. With regard to the identification process, variations are observed at these instants in the estimated parameters of the percentage of solids model, while the estimated parameters of the level model remain unaffected.

Later, at 96 min the level reference decreases from 60% to 40% while coupling in the percentage of solids is not noticeable in Fig. 8, but an overshoot exists in the response of the level. It is appreciated from Fig. 8 that the controller just moves the pump speed. This shows that the speed has a low degree of interaction with the percentage of solids. Small variations are observed in all the estimated parameters during this change with respect to the identification process.

Finally, at 111 min the reference of percentage of solids is decreased from 74% to 72% and a large coupling on the level and, in general the adverse effects of those, is shown in Fig. 8, when the reference of the percentage of solids is increased at $t = 80$ min. From the identification standpoint, only some of the parameters of the percentage of solids model and level model vary. The test concludes approximately at 120 min.

5.4. Multivariable direct Nyquist array control (MDNAC)

5.4.1. Case 1: static precompensator

Using the method described in Section 3.4, the design of a static precompensator was attempted and the corresponding PID controllers were designed using a model of the plant drawn from experimental data. The normalized model turned out to be

$$\mathbf{G}_N(s) = \begin{bmatrix} \dfrac{-2.536}{(1.917s+1)} & \dfrac{1.589}{(2.129s+1)} \\ \dfrac{-0.915(0.327s+1)}{0.774(1.136s+1)^2+(2.549)^2} & \dfrac{-11.305(0.118s+1)}{0.549(1.350s+1)^2+(0.944)^2} \end{bmatrix} \quad (14)$$

The column dominance of $\mathbf{G}_N(s)$ can be appreciated from the DNA plots shown in Figs. 10 and 11.

The static precompensator was designed from the model given by Eq. (14) and has the following form:

$$\mathbf{K}_e = \begin{bmatrix} -0.375 & -1.962 \\ 0.031 & -3.131 \end{bmatrix}$$

The dominance of the columns of the plant together with the static compensator can be seen in Figs. 12 and 13.

The PID controllers for each loop were tuned according to the IMC method [19,20] and the resulting parameters were:

$$\mathbf{C}_e(s) = \frac{1}{s}\begin{bmatrix} 1.043(1.917s+1) & 0 \\ 0 & 27.64(0.025s+1) \end{bmatrix}$$

The strategy was later applied to the CODELCO-Andina grinding plant the results of which are shown in Figs. 14 and 15. Fig. 14 shows the output variables and their references. Less coupling on the level L is observed, when compared with the multivariable sequential loop closing control (Fig. 20), upon changes in the reference of the percentage of solids D. Variable D remains flat upon changes in the level reference. Better stabilization of D certainly exists around its reference value and the response is also much faster.

Fig. 15 shows the control efforts to achieve the control objectives. Much less abrupt variations are observed, when compared with the MSLC control (Fig. 21), but there are larger variations on the sump water flow F in order to satisfy the control objectives for each output variable. The pump speed, S, has a second-order type response and produces significant overshoot.

5.4.2. Case 2: dynamic precompensator

Following the procedure established in Section 3.4 and using the experimentally obtained model described by Eq. (14), the following dynamic precompensator was obtained:

$$\mathbf{K}_d(s) = \frac{1}{(0.667s+1)^2} \times \begin{bmatrix} -0.3748(0.667s+1)^2 & -0.0426(1.909s+1) \\ 0.03112(0.667s+1)^2 & -0.0679(2.122s+1) \end{bmatrix}$$

The column dominance of the plant together with the dynamic compensator is illustrated in Figs. 16 and 17.The

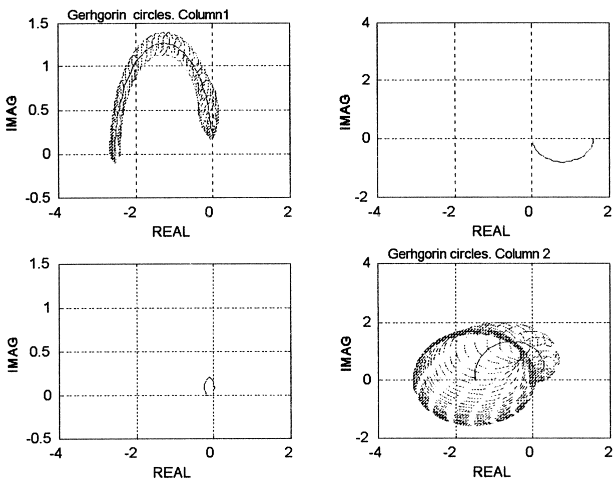

Fig. 10. Nyquist diagram of $\mathbf{G}_N(s)$.

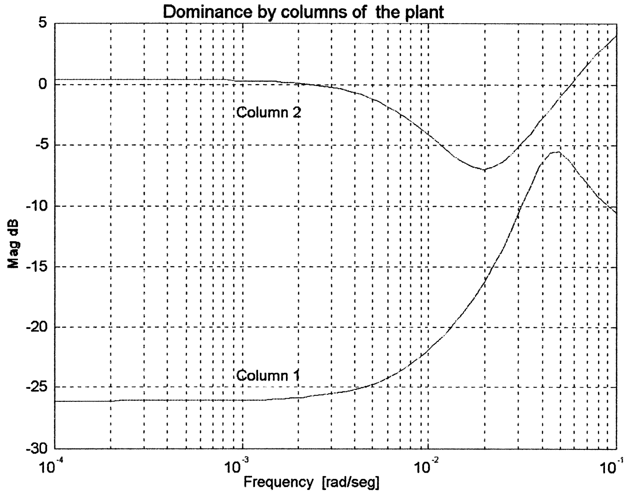

Fig. 11. Dominance by columns of $\mathbf{G}_N(s)$.

adjustment of the PID controller parameters using the IMC method turned out to be:

$$\mathbf{C}_{din}(s) = \frac{1}{s}\begin{bmatrix} 0.338(2.333s+1) & 0 \\ 0 & 77.824(0.017s+1) \end{bmatrix}$$

The control strategy was later implemented in the grinding plant with the results shown in Figs. 18 and 19. Fig. 18 shows the output variables and their references. As in Case 1, reduced coupling on the sump level L are observed with respect to changes in the reference of the percentage of solids D. However, variable D does exhibit variations upon changes in the sump level reference.

5.5. Multivariable sequential loop closing control (MSLCC)

For the sake of comparison, the implementation of a strategy based on two SISO PID controllers was performed. The two control loops selected were the percentage of solids (density) D vs. sump water flow F, and the level L vs. pump speed S. For the L–S loop, the PID configured in the DCS was used which is part of the current control scheme at the CODELCO-Andina grinding plant. The D–F loop is designed according to the MSLC method [1] and the PID control parameters are tuned using the IMC method [19,20]. Final tuning is performed on site during the control test.

The model, obtained experimentally, for D vs. F when the loop L vs. S is closed is given by:

$$g_{df}(s) = \frac{-0.849\,e^{-0.114s}}{3.118(0.3207s^2+0.7142s+1)}$$

Starting from this model a PID controller was designed for the D vs. F loop. The control parameters were chosen such that the controller transfer function is:

$$C_{slc}(s) = \frac{-0.311(0.167s+1)}{s}$$

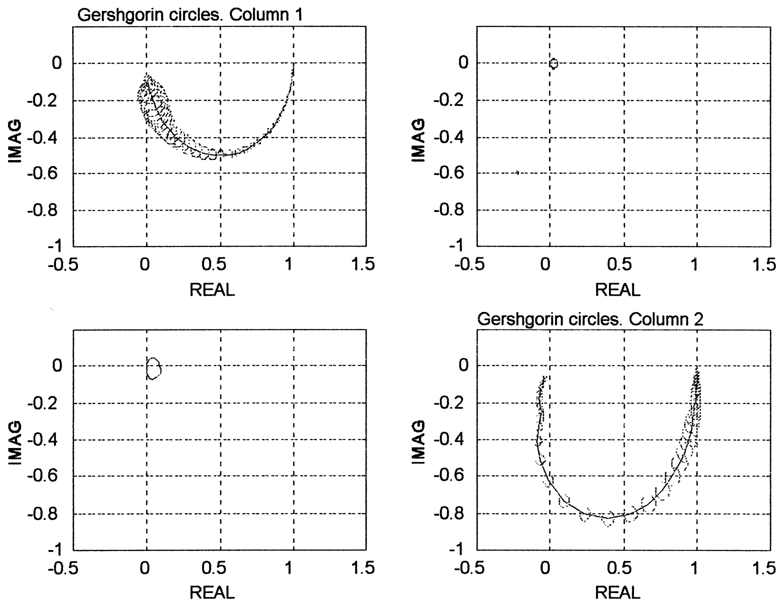

Fig. 12. Nyquist diagram of $\mathbf{G}_N(s)\mathbf{K}_e$.

Later on this controller was implemented in the plant and the results are shown in Figs. 20 and 21. The experiment is described in Table 5 and was conducted on ball mill No. 9.

The test was performed under normal conditions with no unplanned disturbances. And there were no overload phenomena during the test.

The experiment was started and the PID parameters remained constant following a series of preliminary tests to improve the initial tuning of the PID controller parameters in the percentage of solids–pump speed loop.

The experiment is now described chronologically. Initial references values were 74.5% for the percentage of solids and 45% for the level.

At $t = 9$ min, when the reference of percentage of solids is decreased from 74.5% to 71%, the level responds poorly, as shown in Fig. 20, because the coupling effect produces a peak deviation lasting 8 min with an initial

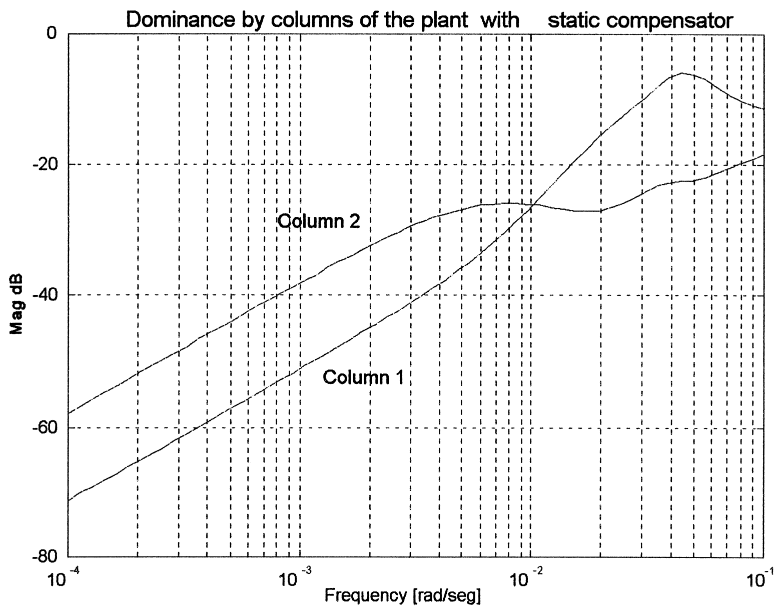

Fig. 13. Dominance by columns of $\mathbf{G}_N(s)\mathbf{K}_e$.

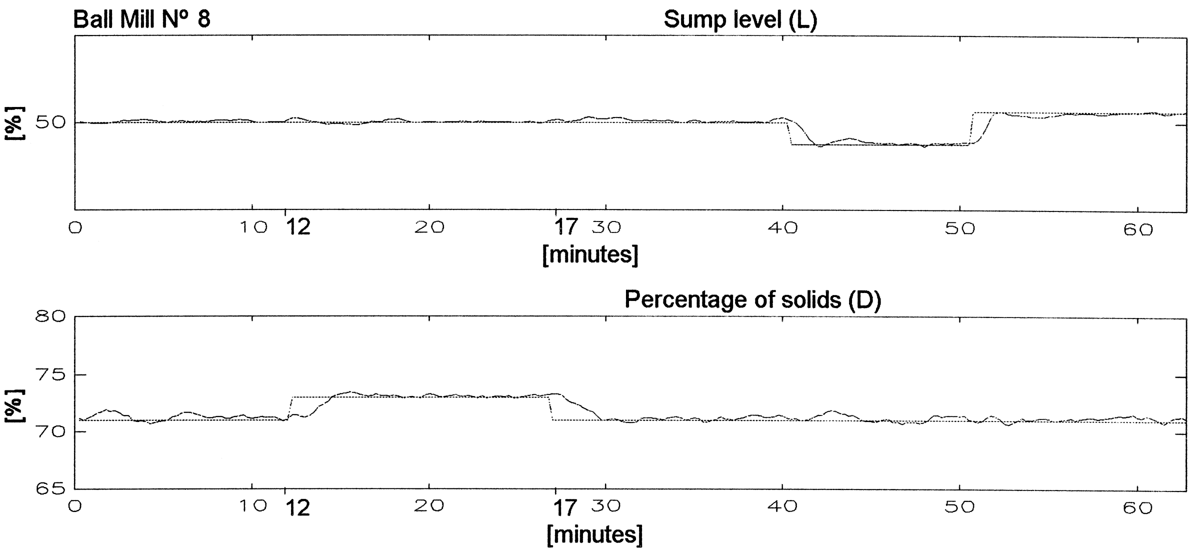

Fig. 14. Controlled variables for the implementation in plant of the MDNAC (static precompensator).

peak of 15%. At $t = 19$ min, when the reference of percentage of solids is increased from 71.5% to 73%, Fig. 20 shows that exhibits strong coupling in the response of the level, although this is less than the previous one as the step change is of smaller magnitude.

In summary, the response of the percentage of solids, assessed independently, is satisfactory, however the sump level exhibits significant perturbations.

At $t = 29$ min, the level reference is changed from 45% to 60% and it is observed in Fig. 20 that there is almost no coupling in the percentage of solids, which is partly due to the nature of the plant. This can be verified by consulting Fig. 21 which shows that the valve opening remains almost constant from $t = 22$ min. The same occurs at $t = 39$ min when the level reference is decreased form 60% to 50%.

Finally, it can be concluded from the large coupling in the level following modifications to the reference of percentage of solids just how important it is to have a good multivariable control strategy.

5.6. Present operation of CODELCO-Andina grinding plant

To get an idea of the behavior of the plant during its present, normal operation, the evolution of the percentage

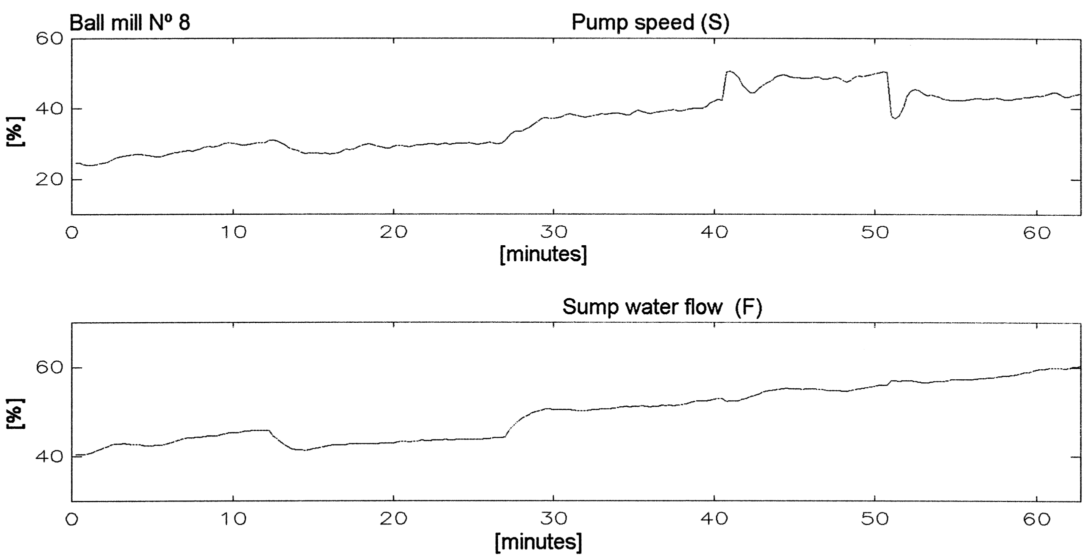

Fig. 15. Manipulated variables for the in-plant implementation of the MDNAC (static precompensator).

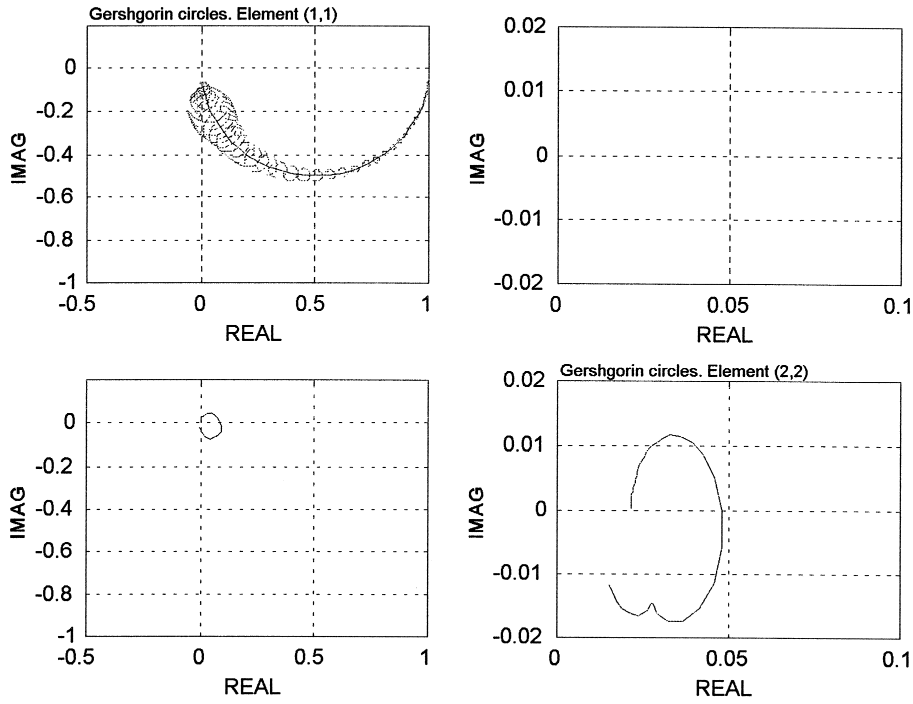

Fig. 16. Nyquist diagram of $\mathbf{G}_N(s)\mathbf{K}_d$.

of solids and of the sump level were registered under current control conditions, i.e., SISO PID control in the loop sump level vs. pump speed, designed by CODELCO-Andina, and with the D vs. F loop open. The test was carried out on ball mill No. 9 and is described in Table 6. Since only a single loop is available (L vs. S), the test simply consists of applying step changes to the valve opening and changes to the level reference.

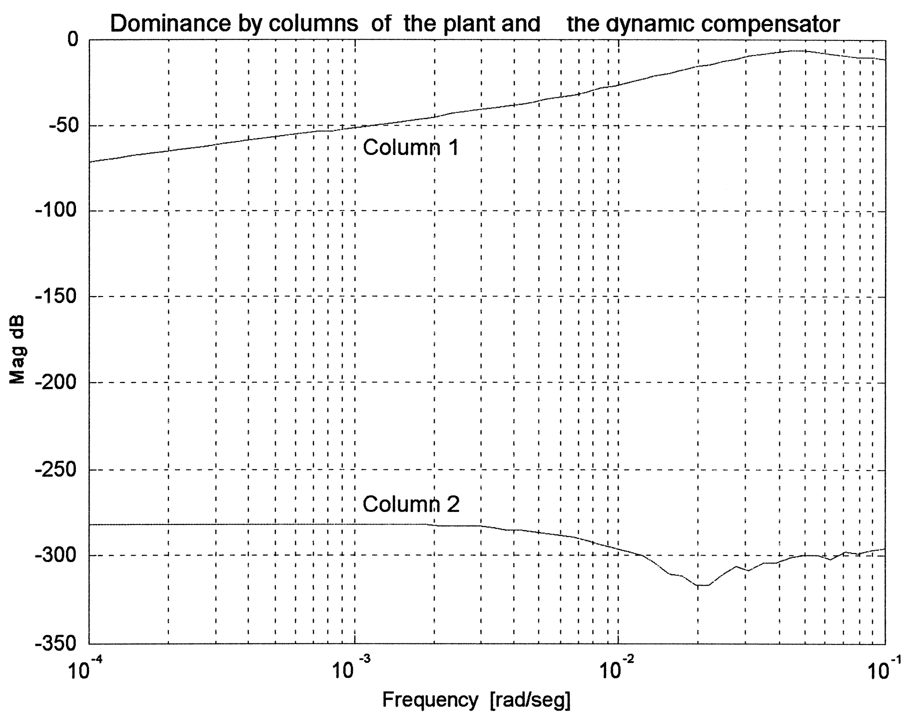

Fig. 17. Dominance by columns of $\mathbf{G}_N(s)\mathbf{K}_d$.

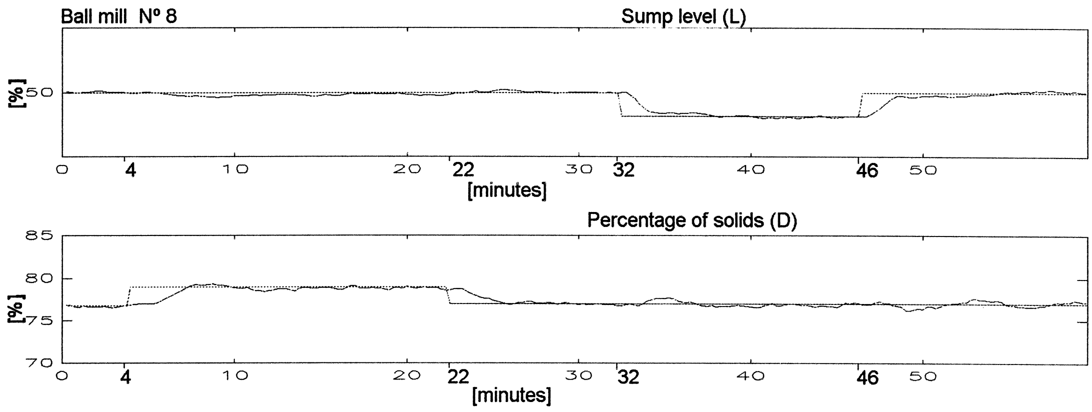

Fig. 18. Controlled variables for the in-plant implementation of the MDNAC (dynamic precompensator).

The test conditions were normal, since no unplanned disturbances of any type were encountered during the experiment. Next, the experiment is described in chronological order.

A large coupling in the level response is shown in Fig. 22, upon changes in the valve opening made at $t = 5$ min and $t = 17$ min from 41% to 35% and from 35% to 42%, respectively. The percentage of solids, on the other hand, slides from 78.5% at $t = 8$ min down to 71% at $t = 20$ min.

At 33 min and 46 min when the level reference is changed from 40% to 60% and back again to 40%, the coupling in the percentage of solids is observable in Fig. 22, and is due to control actions taken on the pump speed. The response of the level deteriorates resulting in a large overshoot.

The step changes in the valve opening and the control actions taken on the pump can be seen in Fig. 23.

The tests described in Sections 5.5 and 5.6 were carried out on the same ball mill using the same PID controller (sump level–pump speed) configured on the DCS. However, on comparison of the responses, they are quite different (Figs. 20 and 22). Approximately a month elapsed between the two tests. The differences in the behavior of the controllers indicates the scale of the variability of the plant and the necessity of a good multivariable adaptive control strategy.

The great variability of the percentage of solids in the pulp feeding the hydrocyclones (which is highly correlated with the +65 mesh particle size in the hydrocyclone overflow), strongly determines the mineral recovery at the output of the flotation stage.

It is appreciated from Fig. 22 that, in the case of the level, the control variable remains stable but oscillatory around its reference. The policy is not to change the reference, but to maintain control by stabilizing the sump

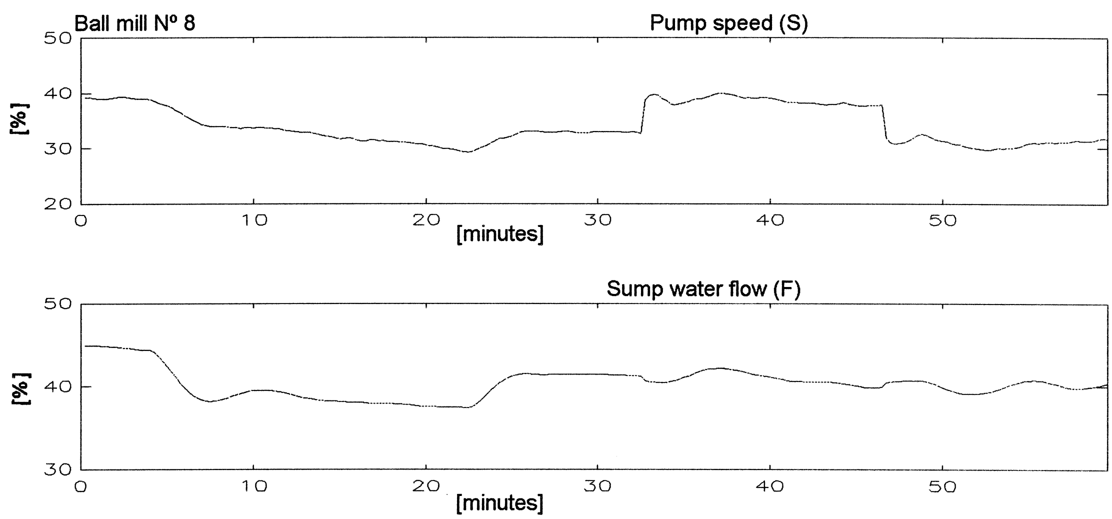

Fig. 19. Manipulated variables for the in-plant implementation of the MDNAC (dynamic precompensator).

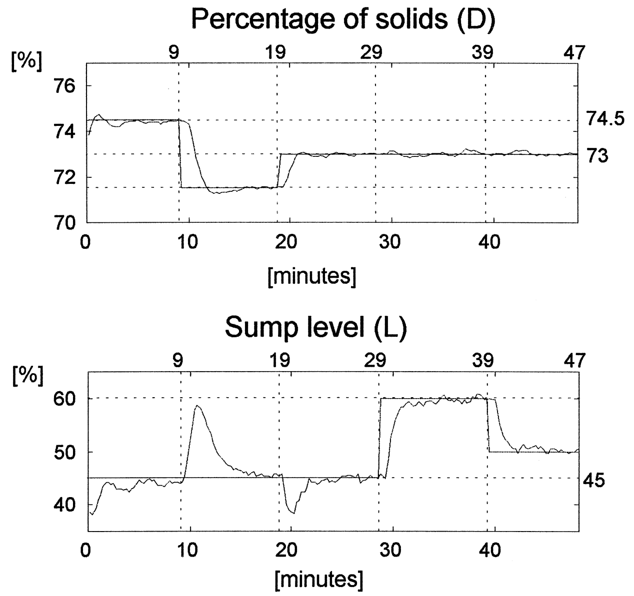

Fig. 20. Controlled variables for the in-plant implementation of the MSLCC.

level. Changes in the level and in the percentage of solids are mainly caused by changes in the water sump. Fig. 22 indicates that it is the sump water which is varied. This happens as the operator tries to maintain the electric power

Table 5
Description of the experiment carried out with two SISO PID controllers

Time interval [min]	Reference of percentage of solids [%]	Reference of sump level [%]
0–9	74.5	45
9–19	71.5	45
19–29	73	45
29–39	73	60
39–47	73	50

of the ball mill within a certain range, to avoid its overloading.

On comparing the classical multivariable strategies and the current operation of the grinding plant, the worst system of the three is Andina's present control system. Any control considering a nondiagonal compensator is better than the single-loop-tuned PID controller. It is also concluded from these tests that even a static compensator improves the system behavior.

6. Comparison and economical aspects

A comparison follows between the multivariable control strategies and the present normal operation of the

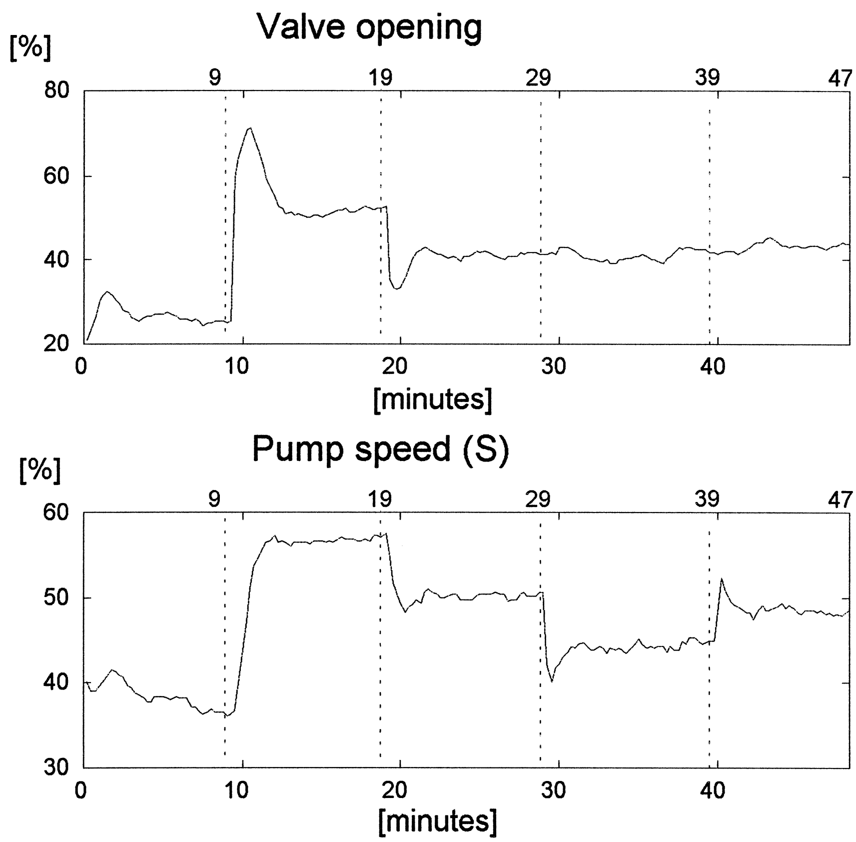

Fig. 21. Manipulated variables for the in-plant implementation of the MSLCC.

Table 6
Description of the experiment performed on the CODELCO-Andina grinding plant under its current control

Time interval [min]	Valve opening [%]	Reference of sump level [%]
0–5	41	40
5–17	35	40
17–33	42	40
33–46	42	60
46–62	42	40

CODELCO-Andina grinding plant. An economic impact analysis of the benefits is carried out to establish the significance of implementing the multivariable algorithms in all three sections of the plant.

6.1. Performance index

The control strategies are evaluated and compared by means of a performance index. A performance index function depending on the tonnage of mineral processed and on the particle size in the overflow of hydrocyclones is proposed in Ref. [34]. However, given that in this case the particle size at the hydrocyclone overflow is unavailable and, that it has been determined that the percentage of solids fed to hydrocyclones is an equivalent measurement of the particle size, an equivalent performance index depending on the tonnage processed and on the percentage of solids is stated. The modified version of the performance index [34], is

$$J = \int_{t_o}^{t_o+T} \left(a\mathrm{Ton}(\xi) - b\left(\mathrm{Cp}(\xi) - \mathrm{Cp}^*\right)^2 \right) \mathrm{d}\xi \qquad (15)$$

where $\mathrm{Ton}(t)$ is the feed tonnage, $\mathrm{Cp}(t)$ is the percentage of solids fed to hydrocyclones, and Cp^* is the optimum (ideal) percentage of solids fed to hydrocyclones. Constants a and b are weighing factors and T is the evaluation horizon.

It is seen that the functional has a maximum when the percentage of solids is closer to its reference and when the processed tonnage is larger. Therefore, the best strategy will be the one that has the larger value of the performance index for a given horizon T.

For the sake of comparison, the performance index is evaluated for the present normal control against the multivariable extended horizon adaptive controller over a period of $T = 85$ min. Only one adaptive strategy is evaluated, since under steady state all three adaptive strategies present similar behavior. The evaluation horizon used in this study is small, because plant availability for this type of test is very limited.

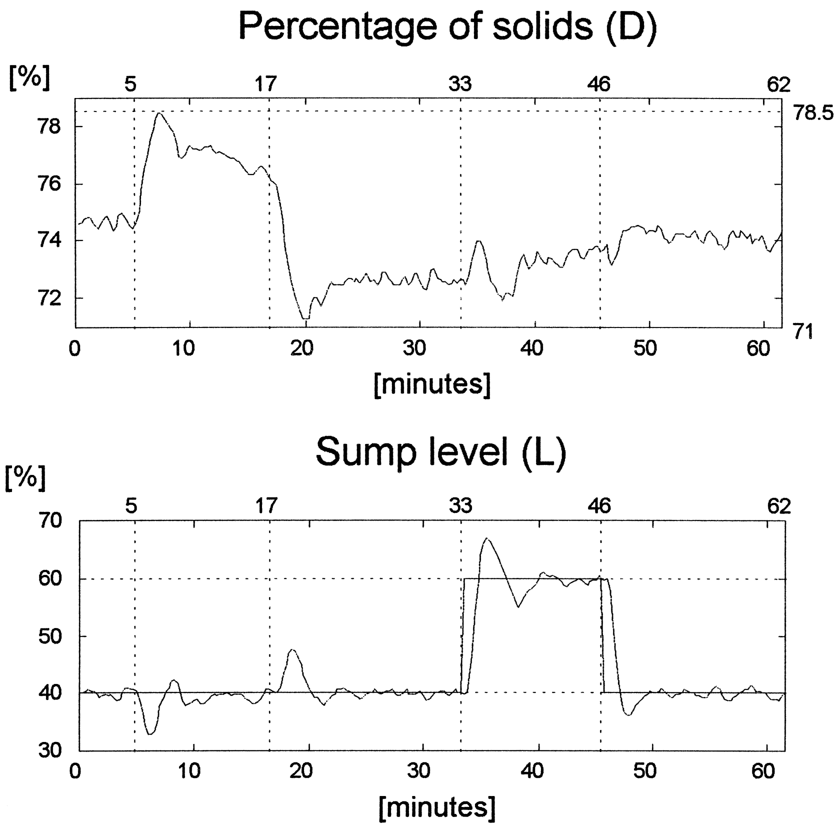

Fig. 22. Controlled variables for the present, normal operation of the plant.

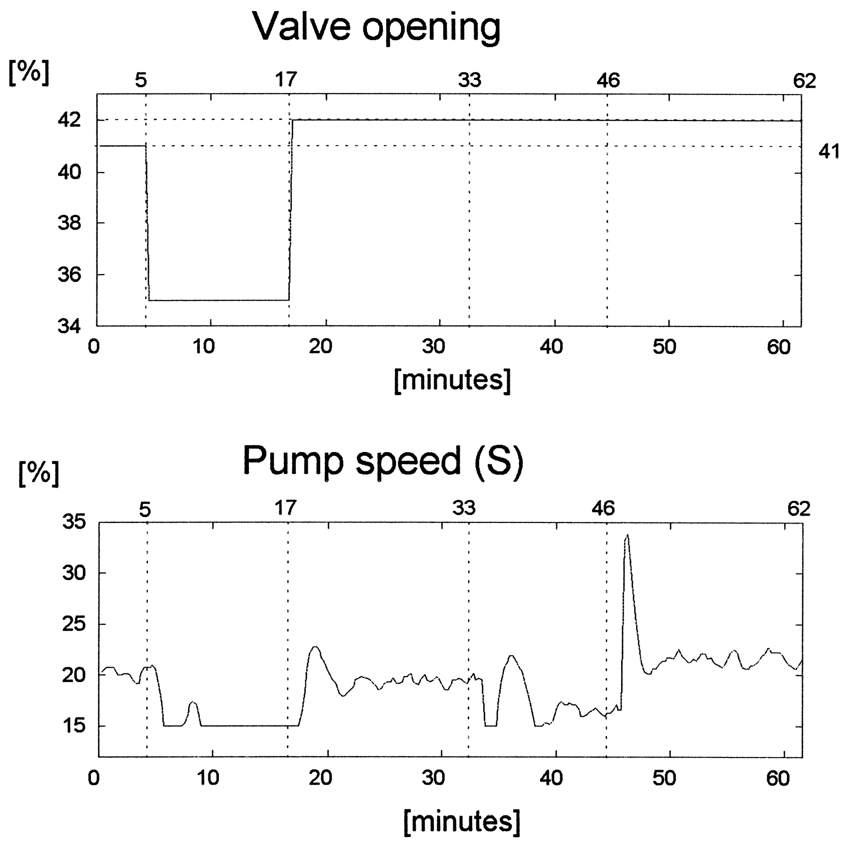

Fig. 23. Manipulated variables for the present, normal operation of the plant.

In this study, the weighting factors used are $a = 1/100$ and $b = 1/10$ [16], to get the performance index to a similar sensitivity for the processed tonnage and for the percentage of solids. It has been determined that the optimum percentage of solids, fed to the hydrocyclones, to obtain good recovery in the flotation stage is $Cp^* = 73\%$.

For the present control at the CODELCO-Andina grinding plant the functional takes a value of $J_1 = 399.21$. For operation under the MEHA controller the functional takes a value of $J_2 = 1595.90$ (see Fig. 25). The tonnage processed in both cases is practically the same. Under current normal operation an average of 470 TPH is processed while under the MEHAC strategy an average of 463 TPH is handled. Therefore, the difference found between J_1 and J_2, is due to the improvement in the control of the percentage of solids and, in consequence, to the particle size.

Another comparison is made between the present normal operation of the plant and the MDNA controller over $T = 62$ min. The values of the functional for the two cases turned out to be $J_1 = 291.4$ and $J_2 = 1203.4$, respectively (see Fig. 26). Once again, the tonnage processed is practically the same, and therefore the difference found in the values of the functional is due to the improvement in the percentage of solids (particle size).

From these two experiments, it can be concluded that with a multivariable adaptive or classical strategy, such as those studied here, it is possible to improve the final product of the grinding stage without a significant sacrifice in the tonnage processed. The net result is that the same amount of pulp goes to the flotation process, but of better quality and therefore the recovery of copper concentrate is higher with a corresponding economic benefit.

6.2. Economic benefits from using a multivariable control strategy

In this section the economic revenues obtained by using one multivariable adaptive control strategy and one multivariable classical strategy, instead of the present, normal control, are estimated for the CODELCO-Andina grinding plant.

The concentrator plant of CODELCO-Andina can be considered as a black box, grinding and separating the mineral from the tail. The grinding and flotation plant is depicted in Fig. 24 with one input and two outputs.

G_A is the tonnage of mineral fed to the plant each day, L_A is the law of the feeding mineral, G_C is the flow of copper concentrate, L_C is the law of concentrate, G_T is the flow of tails and L_T is the law of tails.

The estimation of the benefits is carried out according to the following revenue function:

$$\Delta I = G_A \times \frac{L_A}{100} \times \Delta R \times \frac{100}{L_C} \times P_C \qquad (16)$$

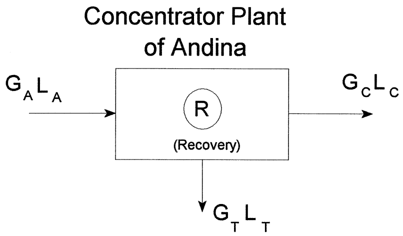

Fig. 24. Schematic diagram of the grinding and flotation plant at CODELCO-Andina.

where $\Delta I = I_{CM} - I_{CA}$, $\Delta R = R_{CM} - R_{CA}$. I_{CM} is the revenue obtained with multivariable control, I_{CA} is the revenue obtained with the actual control of CODELCO-Andina, R_{CM} is the recovery obtained with the multivariable control, R_{CA} is the recovery obtained with the current control of CODELCO-Andina, and P_C is the copper price per ton.

The following values are considered to evaluate the functional Eq. (16): $G_A = 33\,500$ ton/day, $L_A = 1.1\%$, $L_C = 30\%$, $P_C =$ US\$640/ton. In the calculation of the price of the ton of copper concentrate, the average price during 1995 of the copper pound has been used, i.e., US\$1.00.

To compute the value of ΔR the following criteria are used.

(i) The concentrator plant of Andina operates with an approximately constant final law of concentrate and with law of final tail under a certain threshold.

(ii) Given point (i), the metallurgical advantages drawn from grinding much finer product than the optimal value (i.e., $(\% + 65\#)^* = 16.4861\%$ or equivalently $Cp^* = 73\%$) are not completely taken advantage of.

(iii) The metallurgical disadvantages arising from a much coarser grinding than optimal resulting in losses of fine concentrate.

As a consequence of the three previous criteria, optimal recovery of the flotation plant R^* is achieved whenever $(\% + 65\#) \leq (\% + 65\#)^*$ or $Cp \leq Cp^*$. Therefore, higher recovery losses occur when the grinding product is coarse, i.e., when the percentage of solids curve is above the optimal value (Cp^*).

Fig. 25 shows the percentage of solids fed to the hydrocyclones, and the performance against optimum when operating with Andina's current normal control and also under the MAHAC strategy.

Let us define A_{CA} as the area under the curve of percentage of solids $(Cp)_{CA}$ for Andina's current control when $(Cp)_{CA} > Cp^*$, and A_{CM} as the area under the curve percentage of solids $(Cp)_{CM}$ for the multivariable control when $(Cp)_{CM} > Cp^*$.

Let us define T_{CA} and T_{CM} as the time instants corresponding to A_{CA} and A_{CM}, respectively. The total time of the test in each case (with multivariable control and with the current control at the CODELCO-Andina grinding plant) is $T = 85$ min.

The average value of the percentage of solids over Cp^* (i.e., the average value of the percentage of solids corre-

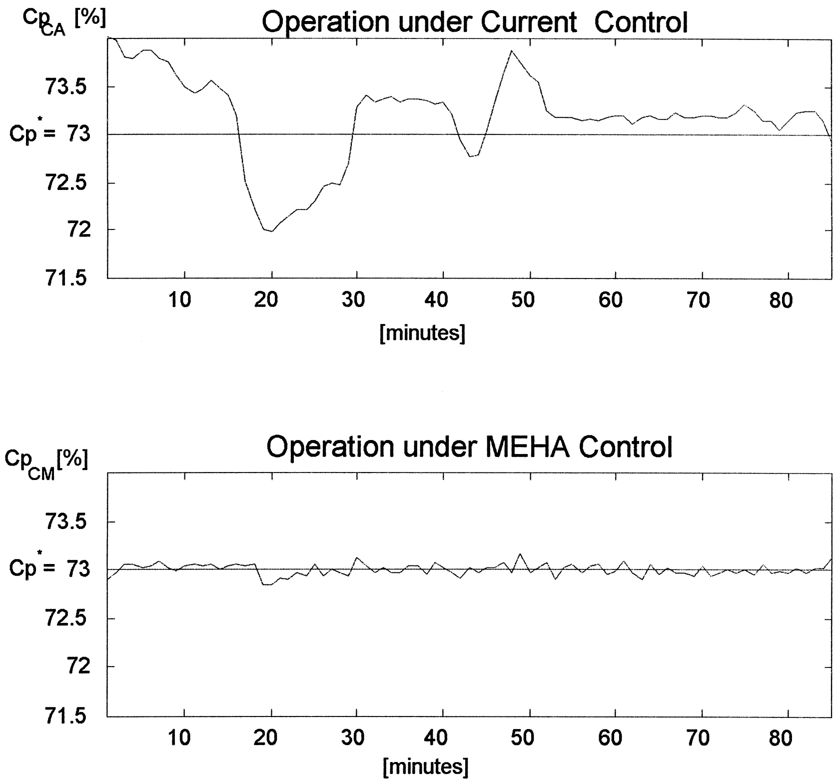

Fig. 25. Comparison between the current control and MEHAC.

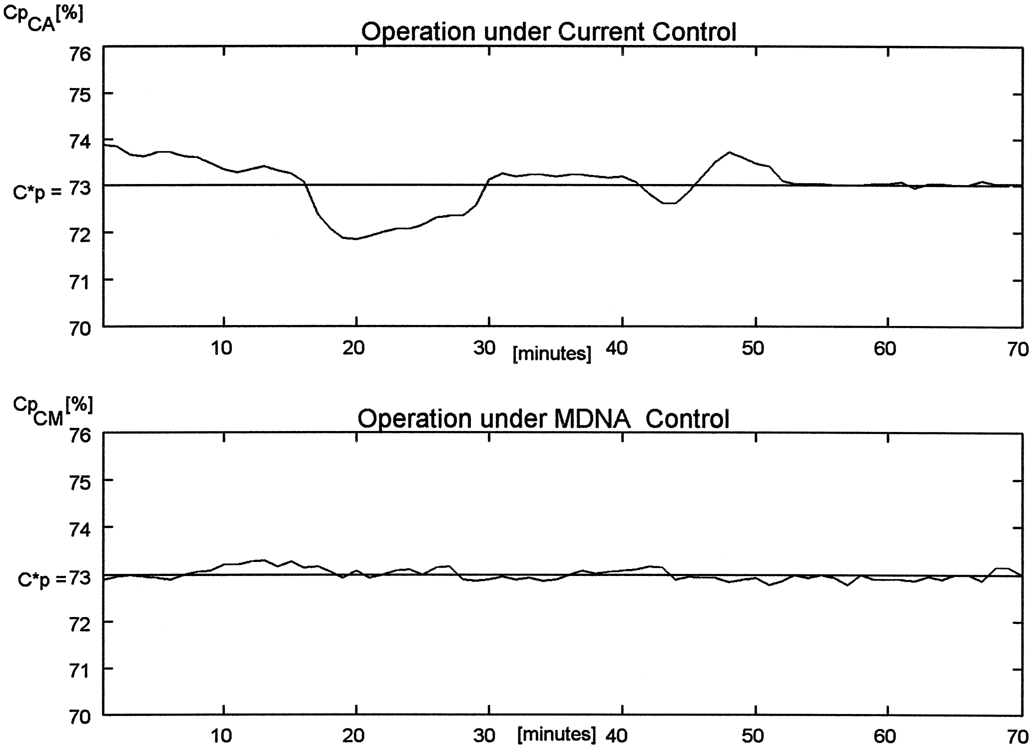

Fig. 26. Comparison of the current operation and control via MDNA for the grinding plant.

sponding to pulp with coarser than optimum particles) is given by:

$$(\mathrm{Cp}_{\mathrm{thick}})_{\mathrm{CM}} = \frac{A_{\mathrm{CM}}}{T_{\mathrm{CM}}} = 73.0457\%,$$

$$(\mathrm{Cp}_{\mathrm{thick}})_{\mathrm{CA}} = \frac{A_{\mathrm{CA}}}{T_{\mathrm{CA}}} = 73.7730\%. \qquad (17)$$

A linear first-order model is obtained from experimental tests and considering the correlation between the particle size and the percentage of solids.

$$(\% + 65\#) = 3.5909\mathrm{C_p} - 245.656 \qquad (18)$$

Therefore, on considering $\mathrm{Cp}^* = 73\%$ and Eqs. (17) and (18), it is possible to obtain the average particle size corresponding to the pulp with coarser than optimum particles (for both control strategies) and also for that corresponding to optimal pulp. These values are:

$$(\% + 65\#_{\mathrm{thick}})_{\mathrm{CA}} = 19.4107\%,$$

$$(\% + 65\#_{\mathrm{thicks}})_{\mathrm{CM}} = 16.7989\%,$$

$$(\% + 65\#)^* = 16.6349\% \text{ (optimum)}$$

Next, the recovery associated with each type of pulp fed to flotation can be computed according to [43] as follows:

$$R = 85.2\left[\frac{240}{-1.776 + 10.072(\% + 65\#)}\right]^{0.083} \qquad (19)$$

Thus we have:

$$(R_{\mathrm{thick}})_{\mathrm{CA}} = 86.7281\%,\ (R_{\mathrm{thick}})_{\mathrm{CM}} = 87.7850\%,$$
$$R^* = 87.8573\% \text{ (optimum)}$$

Therefore, the total recovery for Andina's current control and for the MEHA control are given by:

$$R_{\mathrm{CA}} = \frac{(T - T_{\mathrm{CA}})(R^*) + T_{\mathrm{CA}}(R_{\mathrm{thick}})_{\mathrm{CA}}}{T} = 86.8875\%$$

$$R_{\mathrm{CM}} = \frac{(T - T_{\mathrm{CM}})(R^*) + T_{\mathrm{CM}}(R_{\mathrm{thick}})_{\mathrm{CM}}}{T} = 87.8182\%$$

Finally, $\Delta R = R_{\mathrm{CM}} - R_{\mathrm{CA}} = 0.930\%$ and expression (16) takes a value of $\Delta I = \mathrm{US\$7400/day}$. If the MEHA control system remained in place for 1 year in the three sections of the Andina grinding plant, plant operating improvements could lead to additional annual revenues of US$2 500 000.

Fig. 26 shows the percentage of solids and its optimal value plotted for the current normal operation and under MDNAC.

Carrying out the same previous analysis it is obtained that the average value of the percentage of solids over Cp* are given by:

$$(\mathrm{Cp}_{\mathrm{thick}})_{\mathrm{CM}} = \frac{A_{\mathrm{CM}}}{T_{\mathrm{CM}}} = 73.133\%,$$

$$(\mathrm{Cp}_{\mathrm{thick}})_{\mathrm{CA}} = \frac{A_{\mathrm{CA}}}{T_{\mathrm{CA}}} = 73.276\% \qquad (20)$$

And from Eqs. (20) and (18):

$(\% + 65\#_{\text{thick}})_{\text{CA}} = 18.134\%,$

$(\% + 65\#_{\text{thicks}})_{\text{CM}} = 17.612\%,$

$(\% + 65\#)^{*} = 17.140\%\,(\text{optimum})$

Using Eq. (19) the recovery associated with the pulp fed to flotation stage is given by

$(R_{\text{thick}})_{\text{CA}} = 87.224\%,\ (R_{\text{thick}})_{\text{CM}} = 87.437\%,$

$R^{*} = 87.637\%\,(\text{optimum})$

Then, the recovery, under current normal operation and using the MDNAC, takes the following values:

$$R_{\text{CA}} = \frac{(T - T_{\text{CA}})(R^{*}) + T_{\text{CA}}(R_{\text{thick}})_{\text{CA}}}{T} = 87.242\%$$

$$R_{\text{CM}} = \frac{(T - T_{\text{CM}})(R^{*}) + T_{\text{CM}}(R_{\text{thick}})_{\text{CM}}}{T} = 87.566\%$$

Finally, $\Delta R = R_{\text{CM}} - R_{\text{CA}} = 0.224\%$ and Eq. (16) takes the value, $\Delta I = \text{US\$}1760/\text{day}$.

Additional annual revenue of US$642 740 would be obtained by using MDNA control at Andina instead of its current, normal operation.

Both tests used in this economical evaluation were of short duration and performed under favorable conditions. Therefore, it is reasonable to assume that less benefit would be obtained in more extensive tests. Irrespective, the economic advantages are clear.

7. Conclusions

Five stabilizing multivariable control strategies were implemented as part of an integrated control system in controlling an entire section of the grinding plant of CODELCO-Chile’s Andina Division. The strategies were proven in plant, exhibiting a behavior in line with expected theoretical and previously simulated results.

While the results presented in this paper pertain to the application of multivariable control algorithms on one line of ball mills, the MEHAC and MPPAC strategies have subsequently been proven upon all three lines of Section C simultaneously which produced similar results to those stated here.

The identification algorithm used in the adaptive strategies presents a high degree of adaptability to different types of perturbations. Different values for the nominal memory (S_0) have been proven for the estimator both in plant and in simulations, finding that a poor choice produces a large deterioration in the response of the system, but without losing system stability.

Regarding the in-plant tests, the least satisfactory behavior was obtained with the control system currently in use at the CODELCO-Andina grinding plant, which contains only one control loop.

Extended horizon and pole-placement control demonstrated equally good behavior, however the control actions of the MPPAC are too vigorous and noisy, producing significant wear on the valves. The model reference adaptive control algorithm returned the least appropriate behavior of the adaptive control strategies studied and implemented for this process as it displays pronounced coupling among variables. This method exhibits a further difficulty in its algorithm’s high dependence on the choice of the correction network.

The control methods based on frequency domain, including either a static or dynamic compensator, yield two highly decoupled loops suitable for using two well-tuned SISO PID controllers. On comparing these results with the method of sequential loop closing, that considers a diagonal compensator, better plant control was achieved using a nondiagonal compensator.

The multivariable control strategies studied here are of stabilizing (local) type and form part of an integrated control system which includes an optimizing stage and a supervisory control system, implemented and tested on the CODELCO-Andina grinding plant. These strategies however are not discussed in this paper [48].

Acknowledgements

The results presented here have been supported by CONICYT-Chile, through Grants FONDEF MI-17 and FONDECYT 1950502.

References

[1] J.M. Maciejoswski, Multivariable Feedback Design, Addison-Wesley Publishing (1990).
[2] J.R. Pérez, Implementation of feedforward and multivariable self-tuning controller in chemical process, PhD Thesis, Imperial College, University of London (1987).
[3] P.E. McDermott, D.A. Mellichamp, A decoupling pole-placement self-tuning controller for a class of multivariable process, Proceedings of 9 IFAC World Congress, Budapest, Hungary (1984), pp. 893–898.
[4] V. Hahn, H. Unbehauen, U. Nadolph, Model reference adaptive control of multivariable non-minimum phase pilot plant, Proceedings of 3rd Yale Workshop on Applications of Adaptive Systems Theory (June 1983), pp. 41–46.
[5] G. Metzner, I. McLeod, The application of multivariable adaptive control to an industrial run of mine milling process, Preprints IFAC Symposium on Intelligent Tuning and Adaptive Control, Vol. 4, Applications, Singapore (January 1991).
[6] D. Houdouin, K. Najim, Adaptive control in mineral processing, CIM Bull. 85 (965) (1992) 70–78.
[7] D.G. Hulbert, The state of the art in the control of milling circuits, Preprints of 6th IFAC Symposium on Automation on Mining Mineralogy and Metallurgical Processing, Buenos Aires, Argentina (1989).
[8] K. Rajamani, Self tuning controller of a ball mill grinding circuits, Proceedings of ISA Conference on Instrumentation in the Mining and Metallurgy Industries 12 (1985) 153–159.

[9] P.J. Callaghan, P.L. Lee, Multivariable predictive control of a grinding circuit, Proceedings of 3rd Conference on Control Engineering, Sydney, Australia (May 1986), pp. 99–104.

[10] R. Patel, R. Munro, Multivariable System Theory and Design, Chapter 9: Frequency Domain Design Techniques, Pergamon, London (1981), pp. 237–283.

[11] E. Kelly, D. Spottiswood, Introduction to Mineral Processing, Wiley (1982).

[12] A. Castillo, Multivariable adaptive control applied to mineral grinding (in Spanish), E.E. Thesis, Department of Electrical Engineering, University of Chile, Santiago, Chile (1995).

[13] A. Cipriano, G. Gromsch, Computer multivariable controller design based on frequency methods (in Spanish), Proceedings of the 7th Chilean Engineering Congress, Santiago, Chile, (November 1987), pp. 216–221.

[14] L. Ljung, T. Soderstrom, Theory and Practice of Recursive Identification, The MIT Press, Cambridge (1985).

[15] B.E. Ydstie, L.S. Kershenbaum, R.W.H. Sargent, Theory and applications of an extended horizon self-tuning controller, AIChE J. 31 (11) (1985) 1771–1780.

[16] D.E. Seborg, T.F. Edgar, S.L. Shah, Adaptive control strategies for process control: a survey, AIChE J. 32 (6) (1986) 881–913.

[17] A. Casali, F. Torres, Dynamical grinding simulator for a rod mill in open circuit and ball mill in closed circuit with hydrocyclones (in Spanish), Technical Report MM-3, FONDEF MI-17, University of Chile, Santiago, Chile (1993).

[18] A. Contreras, Multivariable frequency domain control of a mineral grinding plant (in Spanish), E.E. Thesis, Department of Electrical Engineering, University of Chile, Santiago, Chile (1995).

[19] I.-L., Chien, P.S. Fruehauf, Consider IMC tuning to improve controller performance, Chemical Engineering Progress (1990) 33–41.

[20] K. Astrom, T. Hagglund, PID Controllers: Theory and Tuning, 2nd edn., Instrument Society of America (1995).

[21] D.J. Hawkins, Pseudodiagonalisation and the inverse Nyquist array method, Proc. IEE 119 (3) (1972) 337–342.

[22] M.A. Johnson, Diagonal dominance and the method of pseudodiagonalisation, Proc. IEE 126 (10) (1972) 1011–1017.

[23] J.M. Maciejowski, Multivariable Frequency Domain Toolbox User's Guide, Cambridge Control, Cambridge, UK (1990).

[24] J.M. Maciejoswki, New features of the multivariable frequency domain toolbox for MATLAB, in: R. Whalley (Ed.), Application of Multivariable System Techniques (AMST 90) (1990), pp. 1–8.

[25] J.M. Boyle, M.P. Ford, J.M. Maciejoswki, Multivariable toolbox for use with MATLAB, IEEE Control Systems Magazine (January 1989) 59–65.

[26] J.M. Maciejoswki, The Multivariable Frequency Domain Toolbox, MATLAB Toolboxes and Applications, Peter Peregrinus (1993), pp. 1–15.

[27] D.G., Hulbert, J. Koudstaal, M. Braae, G.I. Gossman, Multivariable control of an industrial grinding circuit, Proceedings of III IFAC Symposium on Automation in Mining, Mineral and Metal Processing, Canada (1980), pp. 311–322.

[28] I.J. Baker, D.G. Hulbert, Dynamic behavior in the control of milling circuits, Proceedings of 4th IFAC Symposium on Mining, Mineral and Metal Processing, Helsinki, Finland (1983), pp. 101–115.

[29] G. Metzner, Multivariable and optimizing mill control—the South African experience, Proceedings of 18th International Mineral Processing Congress, Sydney, Australia (May 1993), pp. 293–299.

[30] A. Niemi, P. Heinonen, S.-L. Jamsa, H. Melama, T. Ivarinen, U. Paakkinen, Experiences in multivariable control of sulfide ore grinding in Vuonos concentrator, Proceedings of XIV International Mineral Processing Congress, Canada (October 1982), pp. III 5.1–III 5.12.

[31] A.J. Niemi, R. Ylinen, V. Rasanen, Model based multivariable control of mineral grinding systems, Proceedings of 6th IFAC Symposium on Automation in Mining, Mineral and Metal Processing, Buenos Aires, Argentina (1989), pp. 61–67.

[32] B. León de la Barra, Proposition of a multivariable control scheme for a conventional grinding circuit (in Spanish), E.E. Thesis, Department of Electrical Engineering, Technical University Federico Santa María, Valparaíso, Chile (1988).

[33] A. Cipriano, Reducing the perturbation effects on a linear multivariable system (in Spanish), MSc E.E. Thesis, Department of Electrical Engineering, University of Chile, Santiago, Chile (1973), pp. 319–328.

[34] L.A. Castelli, Design of a control scheme for a section of CODELCO-Andina concentrator (in Spanish), E.E. Thesis, Department of Electrical Engineering, University of Chile, Santiago, Chile (1988).

[35] M.A. Duarte, et al., Multivariable control of grinding plants: a comparative simulation study, submitted to International Mineral Processing (July 1997).

[36] S.-L. Jamsa, H. Melama, J. Penttinen, Design and experimental evaluation of a multivariable grinding circuit control system, Proceedings of the 4th IFAC Symposium on Automation in Mining, Mineral and Metal Processing, Helsinki, Finland (August 1983), pp. 83–91.

[37] J. Koudstaal, D.G. Hulbert, M. Braae, G.I. Gossman, The application of a multivariable controller to an industrial grinding circuit, Proceedings of the 8th IFAC World Congress, Kyoto, Vol. XXII (1991) pp. 210–215.

[38] N. Munro, Recent extensions to the inverse Nyquist design method, Proceedings of the 24th IEEE Conference on Decision and Control (1985), pp. 1852–1857.

[39] M.A. Duarte, A. Castill, F. Sepúlveda, Multivariable extended horizon control applied to a milling plant, Proceedings of the 7th Latinamerican Congress on Automatic Control, Buenos Aires, Argentina, Vol. 2 (1996) pp. 638–643 (in Spanish).

[40] M.A. Duarte, A. Castillo, F. Sepúlveda, Multivariable pole-placement control applied to mineral processing, Inst. Chilean Engineers Rev. 108 (2) (1996) 37–45, (in Spanish).

[41] A. Castillo, F. Sepúlveda, M.A. Duarte, Multivariable adaptive pole-placement control applied to a simulated grinding plant, Proceedings of the Second Latin-American Seminar on Advanced Control, Santiago, Chile, September 26–29 (1995), pp. 165–169.

[42] M.A. Duarte, A. Castillo, F. Sepúlveda, Multivariable model reference adaptive control applied to grinding plants, Inst. Mining Eng. Rev. 52 (218) (1997) 35–45, (in Spanish).

[43] M. Castillo, Prediction of metallurgical results in the CODELCO-Andina copper concentrator (in Spanish), Min.E. Thesis, Department of Mining Engineering, University of Chile, Santiago, Chile (1993).

[44] L.S. Kershenbaum, J.R. Pérez, An extended horizon feedback/feedforward self-tuning controller, AIChE J. 35 (11) (1989) 1835–1843.

[45] D.G. Hulbert, I.K. Craig, M.L. Coetzee, D. Tudor, Multivariable control of a run-of-mine milling circuit, J. South African Inst. Min. Metall. 90 (7) (1990) 173–181.

[46] S.-L. Jamsa, J. Penttinen, H. Melama, Multivariable control design of grinding in Vuonos by inverse Nyquist array, JVTT Research Notes 130, Technical Research Centre of Finland (August 1982), 41 pp.

[47] G.I. Gossman, A. Buncombe, The application of a microprocessor-based multivariable controller to a gold milling circuit, Proceedings of the 4th IFAC Symposium on Automation in Mining, Mineral and Metal Processing, Helsinki, Finland (August 1983), pp. 141–152.

[48] M.A. Duarte, et al., Grinding operation optimization of the CODELCO-Andina concentrator plant, Minerals Engineering (1998), in press.